

**FACULDADE DE ENGENHARIA DA UNIVERSIDADE DO PORTO**



**FEUP** FACULDADE DE ENGENHARIA  
UNIVERSIDADE DO PORTO

# **Myoelectric Prosthesis - Modelization and Control of a Bionic Arm**

**Rafael de Castro Aguiar**

Mestrado Integrado em Engenharia Eletrotécnica e de Computadores

Supervisor: Prof. Fernando Lobo Pereira

April 15, 2015

© Rafael Aguiar, 2015

**MIEEC - MESTRADO INTEGRADO EM ENGENHARIA  
ELETROTÉCNICA E DE COMPUTADORES**

**2014/2015**

A Dissertação intitulada  
“Myoelectric Prosthesis - Modelization and Control of a Bionic Arm”

foi aprovada em provas realizadas em 31-03-2015

o júri

Presidente Professor Doutor José Alberto Peixoto Machado da Silva  
Professor Associado do Departamento de Engenharia Eletrotécnica e de  
Computadores da Faculdade de Engenharia da Universidade do Porto

  
Professor Doutor Joaquim Gabriel Magalhães Mendes  
Professor Auxiliar do Departamento de Engenharia Mecânica da Faculdade de  
Engenharia da Universidade do Porto  
Professor Doutor Fernando Manuel Ferreira Lobo Pereira  
Professor Catedrático do Departamento de Engenharia Eletrotécnica e de  
Computadores da Faculdade de Engenharia da Universidade do Porto

O autor declara que a presente dissertação (ou relatório de projeto) é da sua exclusiva autoria e foi escrita sem qualquer apoio externo não explicitamente autorizado. Os resultados, ideias, parágrafos, ou outros extratos tomados de ou inspirados em trabalhos de outros autores, e demais referências bibliográficas usadas, são corretamente citados.

  
Autor - Rafael de Castro Aguiar

Faculdade de Engenharia da Universidade do Porto



# Abstract

This project concerns the analysis, modeling and control of a prosthetic arm, by means of Electromyographic signals. The social need to fight adversity continuously allows dedicated and innovative studies that aim to achieve new and improved solutions to fight disabilities. The connection between the Biomedical, Mechanical and Electrical Engineering fields becomes more evident, with countless researchers presenting their new ideas and projects in the various fields of biomechatronics.

The project begins with an initial study on the state-of-the-art technologies concerning myoelectric acquisition and processing, and respective control of prosthetic devices. Associated with this study, comes the need to analyze how a real human arm functions, the respective ranges of motion, degrees of freedom, relative weight and segment lengths and normal behaviors in specific case studies. This leads to the design of a somewhat anthropomorphic model in a simulation environment, enabling the replication of the natural limb, by resorting to the Denavit Hartenberg convention for kinematic and dynamic studies, close to those used for normal robotic manipulators.

Another critical feature of this project is to provide a human like behaviour to the simulated limb. To do so, the need to study different control design systems is required. Notions of Hybrid Systems, Nonlinear Control and Model Predictive Control (MPC) are introduced, tools that can in fact provide the desired classes of motion. The selected control architecture is based on MPC, that has the capacity to not only adapt its inputs but its references itself.

The designed system consists in a multilayered control architecture, taking into consideration the human and mechanical constraints, exhibiting 3 separate layers: Motion Planning, Motion Coordination and Low Level Motion Execution Control. The Motion Planning layer receives the processed EMG signal and generates a concatenated set of sub references of the intended motion to be executed. The Motion Coordination layer will include the devised specific MPC adapted controller and adjust the references generated by the higher level. Lastly, the Low Level Motion Execution Control provides all the subsystems with the pre-processed references provided by the MPC. With this architecture, the system provides an extremely "human-like" motion by allowing itself several re planning and adjusting stages.

Several different approaches and redesigns of the control architecture and arm model are performed. A simulation environment is designed to test a 3 degree of freedom arm model (transhumeral type prosthetic), which receives a motion command from a simple control system. The results are compared to a specific case study of a natural, healthy limb with the same movement pattern, yielding a positive response to external disturbances. Due to the limited scope of this project, not all subsystems of the Control Architecture were able to be tested, remaining on a design stage, awaiting further developments.



# Agradecimentos

Antes de tudo mais, ao Professor Fernando Lobo Pereira, por ter ouvido uma pequena ideia e ter ajudado tão fortemente a desenvolver e orientar um fantástico projeto que apenas em sonho se encontrava.

E neste longo percurso, várias foram as fontes de inspiração e ombros amigos que me suportaram, ouviram e choraram/riram a meu lado. Nunca esperei ser tão bem recebido no Laboratório I-109 (Robis) no meio de investigadores fantásticos, de técnicos experientes e de ter saído com inúmeros e incalculáveis amigos e mentores.

Vários são os nomes que gostaria de mencionar ao longo destes meses, porém acho merecerem destaque alguns dos que mais me "aturaram". A ti Daniel, pela tua forte amizade e por me introduzires e encaminhares neste pequeno mundo pós curso.

A ti Jorge e a si Sr. Fernando, por me guiarem e instruírem num mundo técnico para mim novo, pelas histórias fantásticas e sessões de "treino" que me facultaram.

A ti Héber e a ti Filipe, por olharem para mim como um miúdo que precisava de ajuda e logo prontificarem os vossos conselhos, fornecendo também aquela motivação extra no dia-a-dia com a constante pergunta "Já está escrita?".

A ti Diana, por toda a tua ajuda, por todo o teu conhecimento e pela tua amizade fantástica. E a ti minha nova irmã Graça, pelo sorriso que me conseguias dar todos os dias.

Aos meus pais e irmãos, maiores fontes de inspiração da minha vida e alicerces de todo o meu sucesso.

And last, but not least, to you Cécile. Your words and love guide me through the greyest days and give me that needed ember to carry on and achieve whatever dream I have.

Rafael de Castro Aguiar



*"One man's 'magic' is another man's engineering"*

Robert A. Heinlein



# Contents

<b>Abstract</b>	<b>i</b>
<b>Abbreviations and Acronyms</b>	<b>xiii</b>
<b>Glossary</b>	<b>xv</b>
<b>1 Introduction</b>	<b>1</b>
1.1 Goals and Scope . . . . .	1
1.2 Methodology . . . . .	2
1.3 Motivation . . . . .	3
1.4 Document Structure . . . . .	4
<b>2 Myoelectric Systems Overview</b>	<b>5</b>
2.1 Signal Acquisition . . . . .	5
2.2 Myoelectric System Architecture . . . . .	8
2.2.1 Data Segmentation . . . . .	9
2.2.2 Features Extraction . . . . .	11
2.2.3 Classification . . . . .	13
2.2.4 Actuators' Control . . . . .	15
<b>3 Control Background</b>	<b>19</b>
3.1 Hybrid Systems . . . . .	19
3.2 Model Predictive Control . . . . .	22
3.2.1 Linear MPC . . . . .	23
3.2.2 Nonlinear MPC . . . . .	24
<b>4 Anatomical Model Analysis</b>	<b>29</b>
4.1 Anatomy of the Arm . . . . .	29
4.1.1 Average Length and Weight . . . . .	30
4.1.2 Types of Joints and their Functionality . . . . .	32
4.1.3 Range of Motion . . . . .	35
4.2 Movement Analysis . . . . .	37
<b>5 Anthropomorphic Arm Kinematic Modelling</b>	<b>41</b>
5.1 Kinematic Modeling . . . . .	42
5.1.1 Forward Kinematics . . . . .	43
5.1.2 Inverse Kinematics . . . . .	45

<b>6 Problem Statement and Approach</b>	<b>51</b>
6.1 Project Requirements . . . . .	51
6.2 General System Diagram . . . . .	52
6.3 Control Architecture . . . . .	53
6.3.1 Motion Planning . . . . .	55
6.3.2 Motion Coordination . . . . .	56
6.3.3 Low Level Motion Execution Control . . . . .	56
6.3.4 Control Architecture Block Diagram . . . . .	57
<b>7 Simulated System Results</b>	<b>59</b>
7.1 Anatomical and Mechanical Constraints Verification . . . . .	59
7.2 Case Study Arm Model Implemented . . . . .	62
7.2.1 Generation of joint angle references . . . . .	63
<b>8 Conclusions</b>	<b>67</b>
<b>A Appendix</b>	<b>69</b>
A.1 Foward Kinematics Rotation and Translation . . . . .	69
A.1.1 Translations . . . . .	69
A.1.2 Rotations . . . . .	69
A.2 Functional Workspace . . . . .	69
A.3 Case Study Kinematics . . . . .	72
A.3.1 Forward Kinematics . . . . .	72
A.3.2 Inverse Kinematics . . . . .	73
<b>References</b>	<b>75</b>

# List of Figures

2.1	Typical raw EMG signal ([1]) . . . . .	6
2.2	Differential Amplification (from [2]) . . . . .	6
2.3	Influence Factors for Surface EMG sensors . . . . .	7
2.4	Surface electrodes without (left) and with (right) silicone sleeve . . . . .	7
2.5	Myoelectric System Architecture . . . . .	9
2.6	Classification error compared to segment length [3] . . . . .	10
2.7	Windowing Techniques . . . . .	11
2.8	Structure of a time-delayed ANN . . . . .	13
2.9	Multilayer perceptron neural network . . . . .	14
2.10	ANN controller scheme . . . . .	14
2.11	Matrix of MLP expected responses [2] . . . . .	15
2.12	State transition diagram of an FSM controller . . . . .	16
2.13	(A) Prosthetic hand with the feedback system (B) Phantom finger mapping on the amputee (C) Conceptual illustration of the whole system . . . . .	16
3.1	Hybrid System Model of a car with 4 gears (above) and a Computer-Controlled System (below) [4] . . . . .	20
3.2	Principle of Model Predictive Control . . . . .	22
3.3	Block Diagram of a Model Predictive Controller . . . . .	24
3.4	Difference between open-loop prediction and closed-loop behavior [5] . . . . .	27
3.5	Basic NMPC Control Loop [5] . . . . .	28
4.1	Regions, bones and joints of the arm [6] . . . . .	30
4.2	Ball and Socket Joint/Shoulder Joint [7] . . . . .	32
4.3	Shoulder Joint Movements [7] . . . . .	32
4.4	Hinge Joint/Elbow Joint [7] . . . . .	33
4.5	Elbow Joint Movements [7] . . . . .	33
4.6	Pronation and Supination of the Forearm [7] . . . . .	33
4.7	Ellipsoid Joint/Wrist Joint [7] . . . . .	34
4.8	Wrist Joint Movements [7] . . . . .	34
4.9	Range of Motion of Glenohumeral Joint [8] . . . . .	35
4.10	Range of Motion of Elbow and Wrist Joints [8] . . . . .	35
4.11	Anthropomorphic Robotic Arm Workspace [9] . . . . .	36
4.12	Reachable Workspace of Right Arm . . . . .	37
4.13	Marker placement on the upper limb [10] . . . . .	38
4.14	Average joint deviations during hand to mouth/drinking [11] . . . . .	39
5.1	Seven DoF kinematic model of human arm and respective robotic peer . . . . .	42
5.2	Structural scheme of a 7 DoF anthropomorphic arm [12] . . . . .	44

5.3	Fraction of Inverse Kinematics Simulink model . . . . .	48
5.4	"VirtuArm" Inverse Kinematics . . . . .	49
6.1	System Overview . . . . .	52
6.2	Control Architecture Diagram . . . . .	57
7.1	Simulated Prosthetic's Workspace - Distal Perspective . . . . .	59
7.2	Simulated Prosthetic's Workspace - Proximal Perspective . . . . .	60
7.3	Simulated Prosthetic's Workspace Two Dimensional Overview . . . . .	61
7.4	Excerpt of generated .csv file with end-effectors possible positions . . . . .	61
7.5	Structural scheme of a 3 DoF Forearm . . . . .	62
7.6	Forward and Inverse Kinematics, yielding correct results with example joint angle values . . . . .	63
7.7	Elbow, Wrist Yaw and Wrist Roll trajectory during "drinking water" task . . . . .	63
7.8	Natural trajectory of human limb during "drinking water" task . . . . .	64
7.9	Complete "drinking water" task representation . . . . .	65
7.10	Disturbance response in "drinking water" motion task . . . . .	66

# List of Tables

4.1	Average Body Segment Length (in percentage of Total Body Height) . . . . .	31
4.2	Average Body Segment Weight (in percentage of Total Body Weight) . . . . .	31
4.3	Range of Motion in human arm joints . . . . .	36
5.1	DH parameters for a Human Arm . . . . .	43
6.1	Functional and Market/User Requirements . . . . .	52
7.1	DH parameters for 3 DoF Forearm . . . . .	62



# Abbreviations and Acronyms

ANN	Artificial Neural Network
AR	Autoregressive
CMRR	Common Mode of Rejection Ratio
CNS	Central Nervous System
DH	Denavit-Hartenberg
DoF	Degrees of Freedom
EEG	Electroencephalography
EMG	Electromyography
FSM	Finite State Machine
IMES	Implanted Myoelectric Sensors
LMS	Least Mean Square
MES	Myoelectric Signal
MLP	Multilayer Perceptron Neural Network
MPC	Model Predictive Control
NMPC	Nonlinear Model Predictive Control
PID	Proportional, Integrative and Derivative
RoM	Range of Motion



# Glossary

Angle of fiber pinnation	The angle between the line of orientation of muscle fibres and the line of muscle action (i.e. the line of pull of the tendon)
Anthropomorphic	Attribution of human form or other characteristics to anything other than a human being. In this case, to the prosthetic arm model
Bionic	Application of biological methods and systems found in nature to the study and design of engineering systems and modern technology
Circumduction	Combination of abduction, adduction, extension, and flexion, allowing for a circular motion of a limb
Electroencephalography (EEG)	Recording of electrical activity along the scalp. EEG measures voltage fluctuations resulting from ionic current flows within the neurons of the brain
Electromyography (EMG)	Electrodiagnostic medicine technique for evaluating and recording the electrical activity produced by skeletal muscles. EMG is performed using an instrument called an electromyograph, to produce a record called an electromyogram
Intrafascicular	Within a bundle of skeletal muscle fibers surrounded by connective tissue (fascicles)
Physiological	Refers to the normal, healthy operation of your body and its organs
Pronation	Rotation of the hand or forearm so that the surface of the palm is facing downward or toward the back
Prosthetic device	Artificial device that replaces a missing body part, which may be lost through trauma, disease, or congenital conditions
Subcutaneous	Situated or applied under the skin
Supination	Rotation of the hand or forearm so that the palmar surface is facing upward



# **Chapter 1**

## **Introduction**

### **1.1 Goals and Scope**

This dissertation concerns the challenges underlying modeling and control of prosthetic arms. Besides the obvious and extremely interesting challenge this project presents, it is also a theme that regards the improvement on the quality of life of patients with this type of physical disabilities.

This effort is designed to fulfill the requirements of the Master degree to be awarded by the Faculty of Engineering. Moreover, it will serve as basis for future investigation by candidates in this area.

The effort in this dissertation aims at providing a better understanding on the concepts behind the topics previously referred (Biomechatronics), having in mind the investigation of control systems for state-of-the-art prosthetic arms. Moreover, it examines the challenges involved in the design of advanced control systems with a hierachic structure and with a Model Predictive Control (MPC) scheme, which, by combining adaptive and robustness properties, enables prosthetic arms - with a structure much simpler than a real arm - achieve functionalities and performances very close to those of a natural arm.

Thus, a key challenge concerns the careful analysis of natural arms behaviors required to extract motion patterns and, from these, motion requirements for the prosthetic arm. These will be key ingredients to specify a control architecture to endow the prosthetic arm with the appropriate behavioral capabilities. Another key challenge concerns the proper decodification of the myoelectric signals able to discriminate the subtle range of commands required to exploit the wealth of sophisticated behaviors to be performed by prosthetic arm. Finally, another important challenge consists in development an MPC based control architecture which is, on the one hand, endowed with the required properties - position and velocity control accuracy, robustness and adaptivity - and, on the other hand, able to satisfy the real-time requirements underlying the behaviors of a natural arm.

Due to the scope of this project, a tight selection of which challenges are to be addressed is performed, considering as well the background of the project participant, revealing the following areas of focus:

- creation of an anatomically correct kinematic model of the arm/forearm;
- design of a multi-layered control architecture, with motion planning, motion coordination and the low level motion execution control;
- study of a specific movement type and respective acquisition of joint angles data sets and;
- creation of a case study based on the control architecture, natural movement and joint angle data sets, with respective comparison of natural and artificial movements.

## **1.2 Methodology**

The objectives and goals of this project are organized into three major complementary scopes, which require specific approaches and methodologies. These are as follows:

### **1. Anatomical Study and Myoelectrical Systems**

- Determination and study of the body area where the prosthesis will be applied, which arm/forearm muscles might produce the most reliable EMG signals for processing, as well as of which kind of EMG sensors should be utilized;
- Techniques for myolelectric signal processing and interpretation;
- Anthropomorphic arm model analysis and modeling;
- Techniques for identifying natural arm motions and determining the associated motion characterizations in an adequate form to the overall control system.

### **2. Control:** Design of a Control Architecture capable of handling the distinct degrees of motion of the prosthesis by using dynamic systems control techniques. It is crucial that the Control Architecture designed handles the replication of natural-limb type of movements and with acceptable response times

### **3. Simulation:** By using MATLAB, a simulation tool will be developed in order to implement and test the efficiency of the overall system, which includes:

- Model of the prosthetic arm;
- Sets of motion constraints specifying the motion requirements of a natural arm;
- Control Architecture which includes several modules and their coordination systems and;

- Simulation environment centered in the chosen test scenario allowing a proper assessment of the models, control system and of the overall system. To achieve this, the difficulties caused by myoelectric signals and motion perturbations should be easily dealt with in the overall simulation.

## 1.3 Motivation

The interaction between human and machine has always been a topic that generates a great source of curiosity. Concepts of prostheses and orthoses have been around for a long time as humans tried to mitigate the loss of functionalities due to missing or injured limbs with artificial devices, mitigating the loss of functionalities. With the advancements of the technologies associated with this area, new products and new ways to create links between human and robot are being discovered and studied every day.

Since the 1950's, when Jack E. Steele coined the term "Bionics", the study of the connection between biology and electronics has been growing exponentially. Investigations have further developed in the area of Biomechatronics, involving already concepts in the areas of biology, electronics, mechanics, robotics and neuroscience.

Nowadays, one of the main areas of research within Biomechatronics is precisely the development of products to mitigate human disabilities. The invention of robotic organs, namely locomotion organs and upper limbs, has allowed many researchers to bring a new hope for those people who lost their own.

With the association of a responsive element, as a robotic limb, the artificial movement feeling associated with normal prosthetic limbs is avoided, trying to provide the user the feeling that the prosthetic limb is somewhat alive and not merely an lifeless attachment.

With the high level of innovation in this area, new materials are being associated with the prosthesis and orthosis and new control methods are being developed, providing a more "human" range of motions and level of interaction with this kind of equipment.

All these factors and the exciting challenges that they present motivate the research in this dissertation that addresses issues in modeling and control by building on the current state-of-the-art in these fields.

The investigation of advanced control approaches methods and respective implementation in a simulation environment proposed in this dissertation consists in a first step towards a more ambitious goals project with countless possibilities and a chance to further develop into more sophisticated research.

## **1.4 Document Structure**

This dissertation is organized in 8 chapters, each one dealing with a specific part of the project.

This current chapter presents a short background about this theme, serving as a basis to justify the objectives, the motivation and the project.

Chapter 2 presents a general literature review on the state-of-the-art of Myoelectric Systems encompassing different approaches for prostheses control, the sensors involved in each one and several mathematical models. The acquisition, processing and interpretation of the Myoelectric Signal are briefly studied.

In Chapter 3, an analysis on control systems is conducted, presenting models and technologies fit to be integrated in the project.

Chapter 4 concerns an anatomical study of the human arm will be presented, to better understand what the overall system will be required to provide to the user. This specifies the constraints for the design of the overall systems, starting with the arm model and after the verification of the ranges of motion.

Chapter 5, based on the previous anatomical study, concerns the kinematic model of the considered prosthesis device and extracts the elements to be controlled by the low level controllers that will be designed in the project.

Chapter 6 discusses the overall problem statement and the control architecture will be formulated and discussed. Moreover, a detailed analysis of each one of the building blocks of the control architecture and of their interaction is provided. This is tightly coupled with a brief exposition of the underlying background.

In Chapter 7, the results of simulations run with the model and control systems implemented are presented and analyzed.

The final chapter will present the conclusions and possible follow up developments for this project.

# **Chapter 2**

## **Myoelectric Systems Overview**

To better present the technologies and concepts pertinent to this project, this chapter is organized in two separate sub-chapters, with the relevant Signal Acquisition specifications and techniques, including sources of error and Myoelectric Systems Architecture, demonstrating the pathway from acquired signal to generated motion class.

### **2.1 Signal Acquisition**

It is important to refer that EMG signals are not the only signals currently used to control robotic prostheses. This is an area that has received quite a lot of attention and innovation over the past years. Namely, the use of Electroencephalography (EEG), which, unlike EMG, detects voltage fluctuations resulting from ionic current flows within the neurons of the brain instead of electric muscle impulses, usually with sensors located along the scalp. This way, the precision and number of signals collected increases, allowing for higher complexity prostheses but increasing exponentially the complexity of the control models. One of the main areas of innovation with the use of this technology is the possibility to implement a more sophisticated feedback, enabling the user to regain some of his/her lost sense of touch. Although the use of this technology provides a higher interest, the complexity and analysis involved would deem the project undoable for the time period, which makes the EMG signals the ideal and selected ones for the context of this project

In order to understand how a myoelectric signal can be analyzed, it is necessary to understand exactly how it is produced. According to [13], the signal originates from the depolarization and repolarization of the muscle fibers, during a muscular contraction, caused by an ionic current transmitted to those fibers by a nerve's axon, thus creating measurable action potentials. These can be read by electrodes on the skin's surface or by invasive techniques, extracting the signal from within the muscle, using implanted myoelectric sensors (IMES).

The work of [13] shows that no significant difference in the classification accuracy of the signals was detected between surface myoelectric sensors or IMES, which is profitable for this project, given the fact that the implementation of IMES would present a higher degree of difficulty,

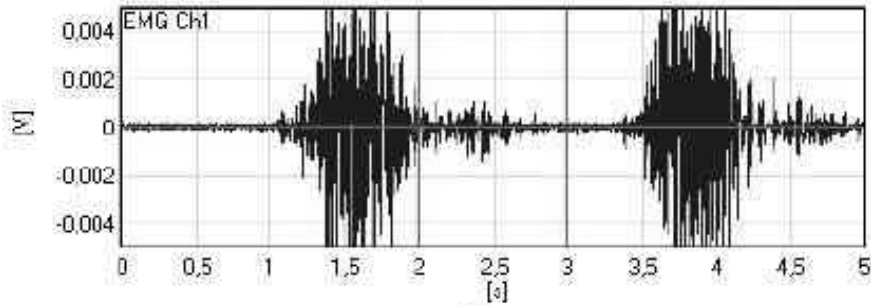


Figure 2.1: Typical raw EMG signal ([1])

which could not be met at this stage. The state-of-the-art surface myoelectric sensors investigated consist mainly of three elements:

- Surface electrodes to acquire the signal (from  $\mu\text{V}$  to mV)
- Differential amplification unit
- Analog to digital converter

Commonly, three electrodes are needed, in order to provide the differential amplification, where two of those act as the positive and negative entries of the amplifier and the third one acts as a reference (Figure 2.2), commonly placed on a bony surface with no significant action potential.

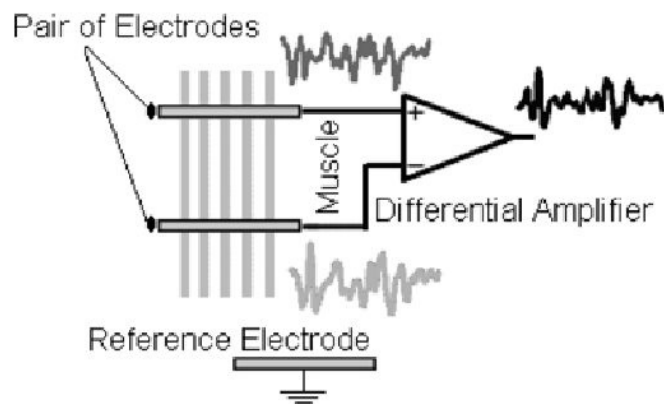


Figure 2.2: Differential Amplification (from [2])

Given the nature of these sensors, they can be susceptible to a variety of error sources. The most common ones are presented by [13], as shown in Figure 2.3 (please refer to the Glossary for specific terms used).

Factors that Influence the Surface EMG			
Nonphysiological		Physiological	
Anatomical	Shape of volume conductor	Fiber Membrane Properties	Distribution of the conduction velocities within the motor units
	Thickness of subcutaneous tissue layers		Distribution of motor unit conduction velocities
	Distribution of motor unit territories in muscle		Average muscle fiber conduction velocity
	Size of motor unit territories		Number of recruited motor units
	Distribution and number of fibers in motor units		Distribution of the motor unit discharge rates
	Length of the fibers		Statistics and coefficient of variation for discharge rate
	Spread of the endplates and tendon junctions within motor units		Motor unit synchronization
	Spread of the innervation zones among motor units		
	Presence of more than one pinnation angle		
Detection System	Skin-electrode contact		
	Spatial filter for signal detection		
	Interelectrode distance		
	Electrode size and shape		
	Inclination of the detection system relative to the fiber orientation		
	Location of the electrodes over the muscle		
Geometrical	Muscle fiber shortening		
	Shift of the muscle relative to the detection system		
Physical	Conductivities of the tissues		
	Amount of crosstalk from nearby muscles		

Figure 2.3: Influence Factors for Surface EMG sensors

An also important error source that can be easily removed is due to the possible alteration in the distance between the electrodes, which can precisely be avoided if, for example, a silicone sleeve fits both electrodes and keeps them in a static place within each other. An example of this application is presented by [2] and can be seen in Figure 2.4.



Figure 2.4: Surface electrodes without (left) and with (right) silicone sleeve

Paired with the electrodes and their amplifiers, it is common practice to insert a filter in the signal before executing the A/D conversion, to initially remove unwanted noise, maintaining the focus in the relevant frequencies of the signal. It is mentioned by [2] that a common source of error for the MES is the electromagnetic induction coming from power lines (50 – 60 Hz), given that the MES has a small amplitude (in the order of micro V to mV), for which the author presents an interesting solution, by inserting a band pass filter, aiming to filter any frequencies below 20 Hz (related to artefact movements and some instabilities in the MES) and high frequencies related to Radio Frequency interference.

A MES' power spectrum is concentrated within a 20 Hz to 500 Hz range (with a full range up to 1 kHz), thus [2] presented solution devises an hardware that uses a second order Butterworth band pass filter with cut-off frequencies of 20 Hz (low) and 1 kHz (high). Having covered both amplification and initial filtering of the signal, it is now necessary to present how to effectively acquire it. To do so, the author of [2] used a simultaneous sample-and-hold data acquisition system, using a high performance acquisition board capable of acquiring multiple channels at high speeds, with 12 bits resolution. Using 5 kHz per channel, the system guarantees that all the components of the MES will be represented (as the Nyquist frequency =  $2 * 500$  Hz). The question at this point remains in the number of channels that will be used for the signal. In the work of [2] 5 channels were used which allowed for 4 different classes of movement: wrist pronation, wrist supination, elbow extension, elbow flexion. For a simple schematic for the acquisition of the MES please refer to the Appendix (A.1).

## 2.2 Myoelectric System Architecture

Knowing now how the MES is acquired, the next task resides in understanding and describing how this signal will be processed and transformed into the data to be fed to the actuators of the motors of the prosthesis. A generic view of the signal processing architecture is presented by [1], which will provide the inputs for the overall control system developed in this project, as can be seen in Figure 2.5.

Myoelectric systems are, in a general basis, mainly composed of four elements (data segmentation, features extraction, classification and control), which range in functions from processing the myoelectric signal and providing, in the end, a reliable control command to the actuators. A generic overview of each of these system sections is presented by [14], describing synthetically each one.

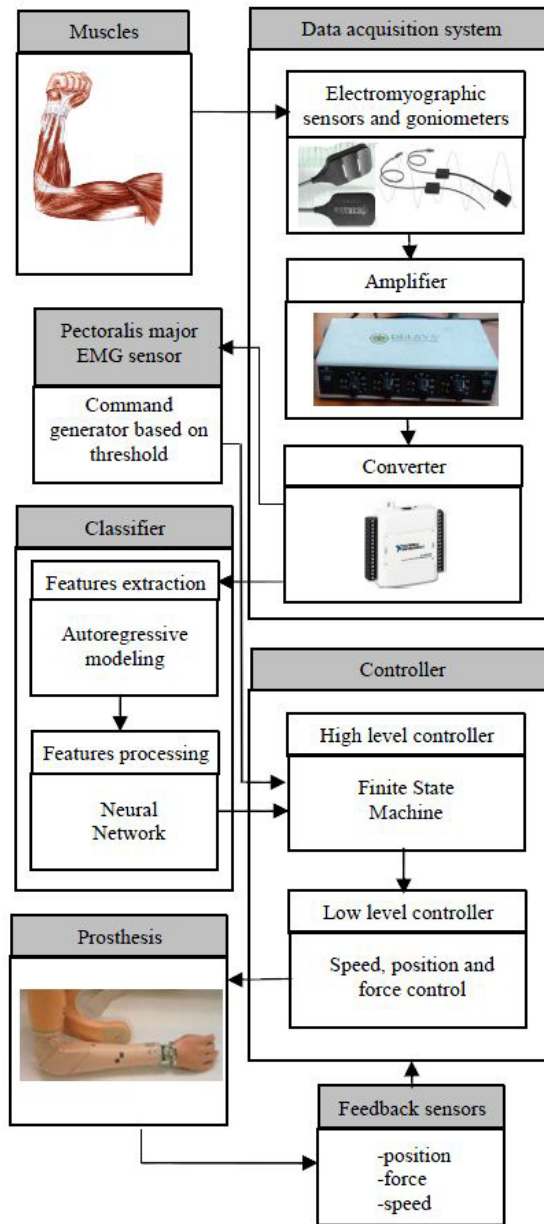


Figure 2.5: Myoelectric System Architecture

### 2.2.1 Data Segmentation

Although the signal is acquired, it is not yet in a state that can be easily read, given the fact that it presents a large number of inputs and has a high degree of randomness. When dealing with continuous signals, it is important and necessary to organize those signals into smaller, individual segments to be able to analyze them properly and, for this case, allow the EMG activity to be reliably represented, which will increase the efficiency of the features extraction from the MES. According to [14], due to real-time constraints, an adjacent segment length plus the necessary the processing time for the signal to generate classified controls should be equal or less than 300

milliseconds. With an increase of the segments length, a decrease on the bias and variance of features is expected, thus improving the classification performance, as can be seen in Figure 2.6.

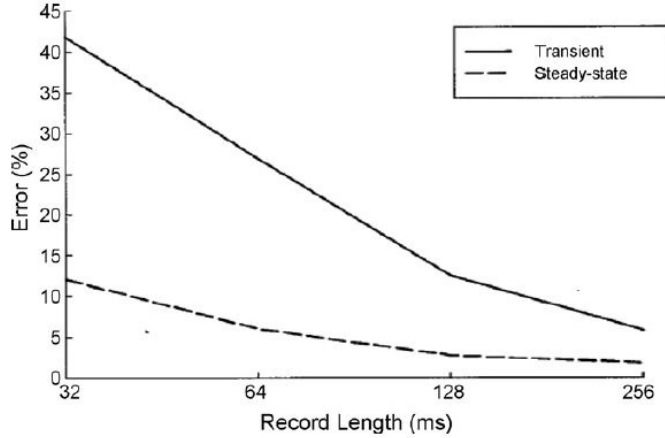


Figure 2.6: Classification error compared to segment length [3]

Although, keep in mind that with higher recording lengths, the delay in the response also increases, generating a higher overshoot. It is also important to refer that a MES contains 2 states: a transient state, in which a muscle goes from rest to a voluntary contraction, thus producing the signal; a steady-state, in which the muscle maintains an already initiated contraction, maintaining the signal already presented.

The transient state, despite having a high capability for classification, has an higher error associated with it, decreasing with the segment length (Figure 2.6), due to the sudden variations. In this case, the fact that the signal is always acquired from a rest position would deem that any action would have to be initiated precisely with the muscle from rest, which prohibits switching from class to class in an effective or intuitive manner and impedes any complex tasks involving multiple degrees of freedom (DOF). Considering this, the author of [14] recommends the use of steady-state segments for the features extraction.

Having considered the segment length and the state of data, a last concept to apply in this data segmentation is the data windowing technique, in order to increase the focus on the precise elements of the segment. Analyzing the work of [14], the respective author presents two different types of windowing:

- Adjacent windowing: adjacent disjoint segments with a predefined length are used for feature extraction and a classified intended motion emerges after a certain processing delay. The processor will only be active during the processing time, remaining idle for the rest of the segment (Figure 2.7 -a);
- Overlapped windowing: unlike the adjacent windowing, the processor will never get into an idle state, using the previous idle times to generate new classified signals (Figure 2.7 -b);

Although the overlapped windowing might provide better accuracy to the system with the increased number of classified signals, [14] presents results from another study that for segments smaller than 125 milliseconds long, high variance and bias in the frequency domain frequencies occur and these segments merely increase processing time without providing any significant improvement in the accuracy of spectral features, such as Autoregressive coefficients, which will be discussed in the next element. Another interesting approach to this concept was presented in the work of [2], in which the authors apply a rectangular window of 200 milliseconds (function returns zero for any element that is outside the selected window) to identify the beginning and end of the signal, removing any inactive segments.

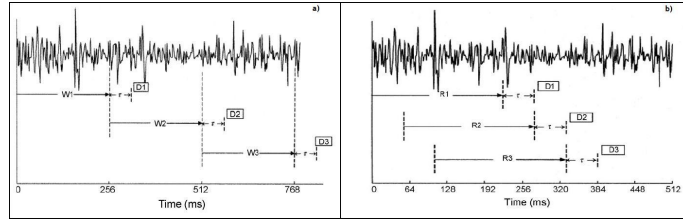


Figure 2.7: Windowing Techniques

### 2.2.2 Features Extraction

Being one of the most critical aspects of myoelectric control, this element analyzes the selected MES segments and extracts their most effective features, in order to provide clear data for the Classifier. The research done presents a number of different techniques to do so. In the survey presented by [14], two methods, based on time-frequency representations are demonstrated, using structural analysis or phenomenological approaches, methods that are also mentioned by [15]. A quite extensive study on the features to be extracted is presented by [16], in which the author describes different approaches, mostly defined in the frequency and time-frequency domain. A few examples, that can be seen in most studies reviewed are:

- *Integral of Absolute Value of the EMG (IAV):*  $IAV = \frac{1}{N} \sum_{i=1}^N x_i$
- *Variance (VAR):*  $\frac{1}{N-1} \sum_{i=1}^N x_i^2$
- *Wavelength:*  $W(n) = \sum_{i=n-N+1}^n |\Delta x_i|$

These three are metric features of the myoelectric signal. For a more complex type of features, that allows a bigger definition of the signal, the use of auto regressive (AR) algorithms is proposed and explained, as shown in [1] and [2]. The AR algorithms are filters that transform the original signals into simpler ones, defined by recursive processes with a small number of coefficients. By the analysis of the previously mentioned documents, the use of an AR algorithm seems to provide

better results, resulting in a more effective classification of the signals, by being simpler to process and reducing this processing time to a minimum. Two of the strongest features of the application of an AR method reside in the fact that, small alterations on the position of the sensors will not have a great impact on the coefficients and, has mentioned before, due to the small number of coefficients, the information to be presented to the classifier will be reduced, reducing as well the processing time required.

The AR model studied is presented by [2]:

$$\hat{y}(n) = \sum_{m=1}^M a_m(n) \cdot y(n-m) + e(n) \quad (2.1)$$

Where:

- $\hat{y}(n)$ : estimated signal in a discrete time n;
- $a_m$ : AR coefficients;
- $e(n)$ : estimated error;
- $M$ : order of the model;

The referred author also presents the steps that were taken to calculate the AR coefficients, based on Least Mean Square (LMS) method:

1. Initialize the filter coefficients with zeroes;
2. Calculate the predicted value of the input signal:

$$\hat{y}(n) = \sum_{m=1}^M a_m(n) \cdot y(n-m) \quad (2.2)$$

3. Estimate the prediction error:

$$e(n) = y(n) - \hat{y}(n) = y(n) + a_1(n-1) + a_2(n-2) + \dots + a_M(n-M) \quad (2.3)$$

4. Update the AR coefficients using the constant of convergence  $\mu$ :

$$a_m(n+1) = a_m(n) - 2\mu \cdot e(n) \cdot y(n-m) \quad (2.4)$$

Regarding the convergence constant, there isn't an ideal value for it, although, [2], based on the experience of other researches, mentions that the use of a very small positive value is advised (approximately 0.001), providing noticeable improvement when the LMS algorithm showed very small errors when processing the whole EMG data set. Although this solution presented itself

valuable, the use of such a small convergence constant brought some minor errors later on, in the Classification element, generating some distortion at the beginning of the EMG activity. To correct this situation, [2] implemented a new strategy, iterating the LMS algorithm as a whole, in which, in the first iteration, the AR coefficients were still initialized with zeroes and in the following iterations, the AR coefficients were initialized with the previous AR coefficients, instead of zeroes, continuing this process until a maximum number of iterations is reached or a minimum error between the estimated and real values of the signal.

### 2.2.3 Classification

With the desired features extracted, it is now necessary to integrate them into distinctive classes for the recognition of the desired motion patterns. According to [14], a problem that presents itself is the fact that, due to the nature of the MES, variations in the values of a particular feature are to be expected. To cope with this, the Classifier needs to be able to adapt to varying patterns and still provide a fast response, in order to meet the real time constraints. There are several methods proposed to perform this classification, using fuzzy models, neural networks, statistical models, Bayesian models and even hybrid ones, mixing, for example, fuzzy and neural networks, which are explained by [14]. One of the most successful methods presented is the use of artificial neural networks (ANN), being able to process linear and non-linear relationships and still meet the time constraints. An example of a time-delayed ANN, containing both feature extraction and classification is presented by [17] (Figure 2.8):

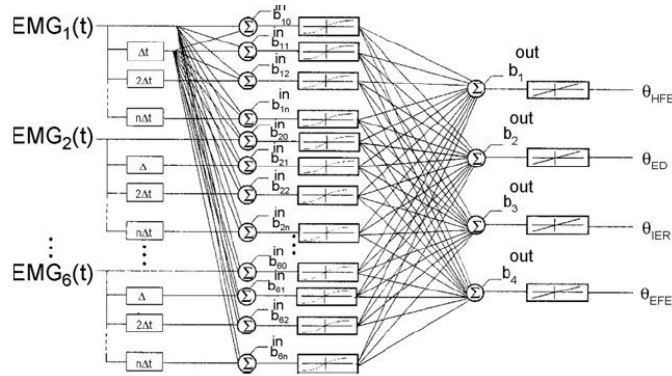


Figure 2.8: Structure of a time-delayed ANN

Although, the implementation of such a complex model raise some difficulties, despite the advantages that it might bring. With that in mind, a unique system to deal solely with the classification seems to render better results. Such a model is implemented in the work of [2], where a Multilayer Perceptron (MLP) neural network is implemented (Figure 2.9), solution which was already explored in other similar projects.

The use of an ANN implies a training stage of that network (see Figure 2.10). To do so, [2] presents a backpropagation algorithm, which is a standard method for training a MLP neural network.

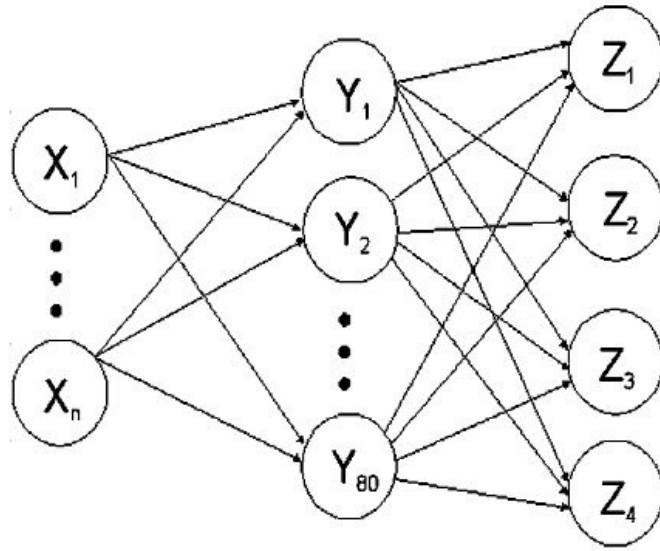


Figure 2.9: Multilayer perceptron neural network

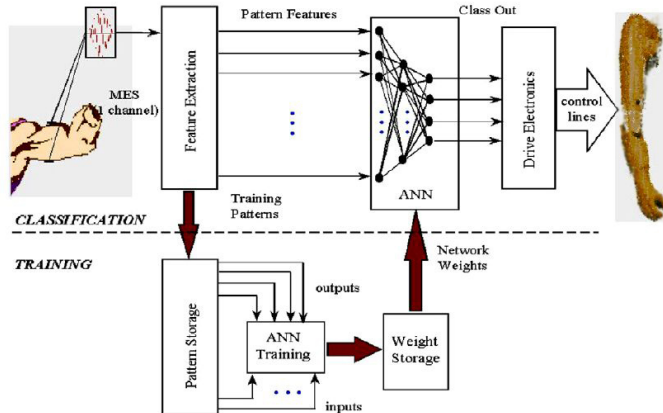


Figure 2.10: ANN controller scheme

This neural network presented is composed of  $n$  neurons in the input layer (where  $n$  is the number of AR coefficients of the previous element), 80 neurons in the hidden layer and 4 neurons in the output layer, which correspond to each movement class defined by the author (elbow flexion and extension, wrist pronation and supination). There is no clear algorithm to define the number of neurons present on the hidden layer, resulting in a more trial-and-error/empirical selection. For this project, the author conducted several experiments with different configurations until an acceptable response was provided. Also regarding hidden layers, an MLP topology may contain several of those, although, as mentioned by [2], according to the Universal Approximation Theorem, demonstrated in the work of [18], only one hidden layer is enough to guarantee the convergence of the MLP training. Having established the model, the completion of the classifier integrates two phases: the training phase, in which several patterns for each class of movement will be fed into the

MLP; execution/test phase to analyze the correct responses of the model. To do so, it is crucial that a correct configuration of the network is met and enough successful training is provided, without overtraining the network though. For the work of [2], the author uses two alternative stopping criteria for the training stage: a total mean square error of 0.01 is achieved; the training will be stopped after 100 epochs. The remaining parameters established for the training stage were: a fixed learning rate of 0.01 and a fixed momentum of 0; a binary sigmoid activation function for all layers; random weight initialization (between 0 and 1) and random presentation of the training patterns; target vectors. The responses expected are presented in Figure 2.11:

Class of movement	Desired network's response			
Elbow extension	1	0	0	0
Elbow flexion	0	1	0	0
Wrist supination	0	0	1	0
Wrist pronation	0	0	0	1

Figure 2.11: Matrix of MLP expected responses [2]

Using this configuration, the authors achieved surprising mean rates of success between 95% and 96%, when using AR coefficients with an order between 4 and 10, so, once more this method becomes attractive to implement in this type of project.

#### 2.2.4 Actuators' Control

The controller's objective is to provide the output commands to the actuators of the prosthesis by “translating” the classifier outputs.

This element provides perhaps the highest degree of freedom, enabling a different array of possible responses. Different kinds of feedback elements can be inserted, so the chance for improvement in this element is always present. In higher complexity projects there can already be seen re-innervation techniques that allow a more “human-like” feel and the regain of touch. A possible high-level controller is presented in the work of [1] (Figure 2.12), where the author implemented a finite state machine (FSM), after implementing a neural network classifier.

This specific controller was created for a three joint upper-limb prosthesis, prepared to work with six movement types: elbow flexion and extension, hand pronation and supination, close and open hand; the “modes” presented in Figure 2.12 are related to the origin/channels that produce the MES and thus correspond to different elements for the classifier. Associated with the FSM, a low-level controller was also devised to efficiently handle force, speed and position variables associated with the prosthesis movements.

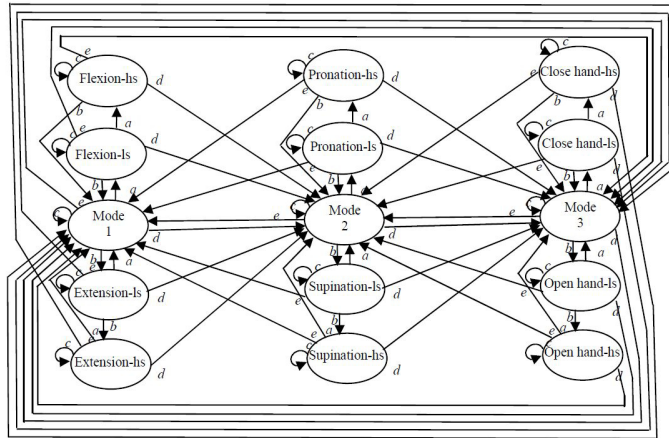


Figure 2.12: State transition diagram of an FSM controller

The final essential aspect of the controller is that the feedback provided has to allow an increase in the controllability and dexterity of the users, without presenting itself as a nuisance. The research conducted brought up a couple of elements that require proper feedback (force, speed and position) and curious techniques used to provide it. Ranging from complex ones, as mentioned previously, by muscle re-innervation where lost or damaged nerves exist, to simpler ones like visual feedback for the force/pressure variable, presenting different colors according to the pressure being applied by the prosthesis in a random object. A more complex research [19] designed a sensory feedback system where the finger tips sensation was mapped into the patient's forearm, by air-mediated pressure, restoring the patient's individual fingers sensation. This mapping is presented in Figure 2.13

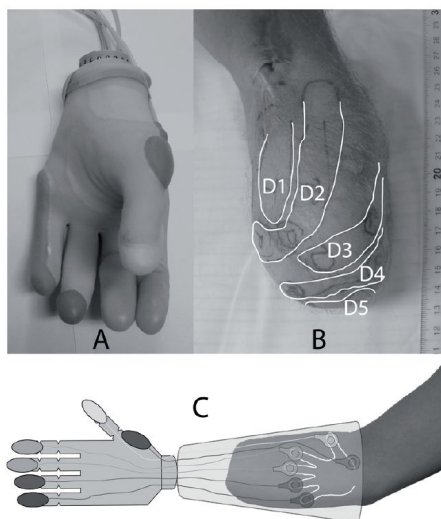


Figure 2.13: (A) Prosthetic hand with the feedback system (B) Phantom finger mapping on the amputee (C) Conceptual illustration of the whole system

Please note that the controller reviewed in this section will be highly different from the one proposed for the project at hand, in notion and application. In this case, the "controller" consists in the system that generates signals to the actuators directly from the results of the Classifier and the interpretation of the MES. Learning methods are implemented to obtain the desired results without the use of models, thus presenting direct feedback without taking into consideration the mechanical model of the prosthetic device itself.

This is where this project aims to improve and innovate. By using the mechanical models, the proposed control architecture aims to decrease the load from these learning processes, in respect to the actuation of the device, presenting more stable and accurate responses. The segment of classification is suppressed and this task is performed by the Control Architecture itself.



# Chapter 3

## Control Background

A bionic prosthetic limb is basically a robotic manipulator that approximates a humanoid limb and its type of behavior. With that in mind, using the Denavit-Hartenberg (DH) parameters, a model of an anthropomorphic limb can be devised.

Although, unlike a normal robotic manipulator, the control of a prosthetic limb isn't, by all means, linear and is required to be able to withstand brute and unpredicted changes while maintaining an acceptable response.

Considering these constraints, this chapter aims to present several Control related tools and concepts capable of providing benefit to the project.

### 3.1 Hybrid Systems

To better understand what an Hybrid System encompasses it is necessary to initially consider the following: a *Discrete System* is a system with a countable number of states, for example, a computer program that may even possess a large state space, will not only be countable but knowingly will be finite; as for *Continuous Systems*, these are systems that present a continuous behavior, normally ruled by a time variable, and that have a real-valued state space, where the system's evolution over time can be described by a continuous function or differential equations.

An Hybrid Dynamic System consists in a dynamic system driven by both ordinary differential equations (time-drive component) and by discrete events. This is a class of systems whose importance has been increasing in engineering due to the fact that the complexity inherent to the modern advanced engineering systems involves not only the laws of physics but also logic. A combination of both Continuous and Discrete behaviors is, for example, a physical system being controlled by a discrete controller (see examples in Figure 3.1).

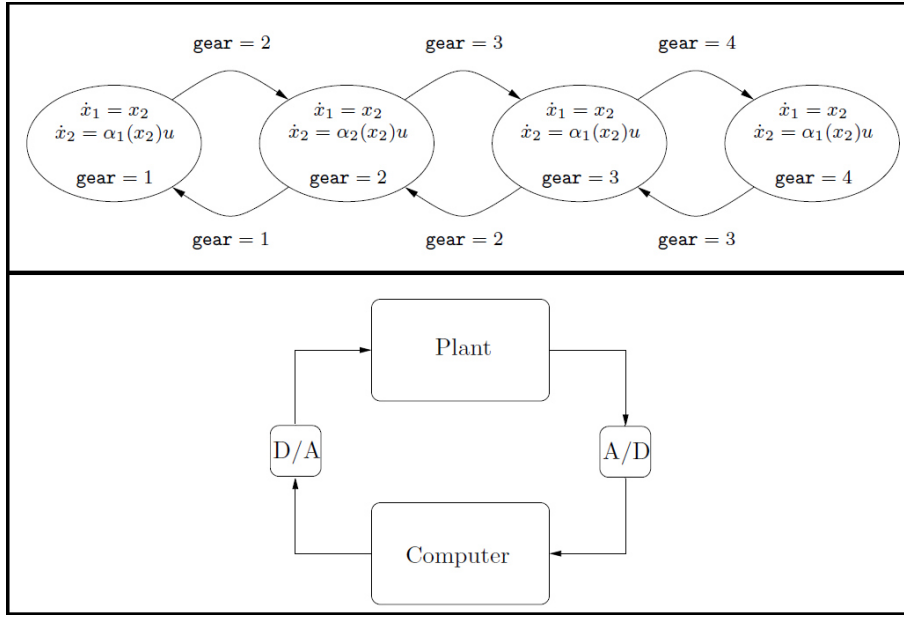


Figure 3.1: Hybrid System Model of a car with 4 gears (above) and a Computer-Controlled System (below) [4]

Among the various types of models to represent this class of systems, *Hybrid Automata* have been the ones gaining the most popularity. In his work, [4] presents this modeling language that describes the evolution in time of the values of a set of discrete and continuous state variables. So, in order to properly define an hybrid automaton, the following elements must be presented:

- $Q \rightarrow$  set of discrete states;
- $X \rightarrow$  set of continuous states;
- $f(.,.) : QX \rightarrow$  vector field;
- $Init \subseteq Q * X \rightarrow$  set of initial states;
- $Dom(.) : Q \rightarrow P(X) \rightarrow$  domain ( $P(X)$  represents a powerset containing all subsets of  $X$ );
- $E \subseteq Q * Q \rightarrow$  set of edges;
- $G(.) : E \rightarrow P(X) \rightarrow$  set of edges;
- $R(.,.) : E * X \rightarrow P(X) \rightarrow$  reset map;

The hybrid system is this way defined by  $H = (Q, X, f, Init, D, E, G, R)$ , in which  $(q, x) \in Q * X$  is a state of  $H$ . The modeling of the system also defines possible evolution for it's state. Considering an initial value  $(q_0, x_0) \in Init$ , the coninuous state variable  $x$  evolves according to the differential equation:

$$\dot{x} = f(q_o, x), x(0) = x_0$$

while the discrete state variable  $q$  remains unchanged:

$$q(t) = q_0$$

The evolution of the continuous component will proceed as long as  $x$  remains within  $\text{Dom}(q_0)$ . In case the continuous state  $x$  reaches the guard  $G(q_0, q_1) \subseteq \mathbb{R}^n$  of an edge  $(q_0, q_1) \in E$ , the discrete state may change its value to  $q_1$  and, subsequently, the continuous state gets reset to a value defined in  $R(q_0, q_1, x) \subseteq \mathbb{R}^n$ . Prior to a discrete transition, the continuous evolution resumes and the process repeats.

Associated with these systems are several constraints that require to be analyzed for an optimal performance. Conditions associated with continuous and discrete systems are naturally transposed to an hybrid system and require, in the modeling stage, to be taken into consideration. The presence of dead-locks associated with the discrete systems, where the operation is locked within a untransitionable state for absence of transition conditions or the Zeno phenomenon, in which an infinite number of discrete transitions occur during a finite period of time, are but a few of the concerns that need to be recognized.

A few of the conditions required to be met at the modeling stage of hybrid systems are presented in [4]:

- *Existence* of solution, precisely taking into consideration the case of dead-locks;
- *Uniqueness* of solution which, if isn't met, imposes to the system a decision between different alternatives. A few measures can be taken in said situations, where different decisions have different priorities;
- *Reachability* which, in rough terms, defines if a state is reachable from any system condition within a finite time period;
- *Verification* which is an important operation that ensures the logic correctness of the behaviors, guaranteeing that the hybrid system meet the desired specifications;

## 3.2 Model Predictive Control

Model Predictive Control was already mentioned a few times before in this report. The objective of this section lies precisely on the description of how this type of controller functions and why is it considered to be a perfect fit for the project at hand.

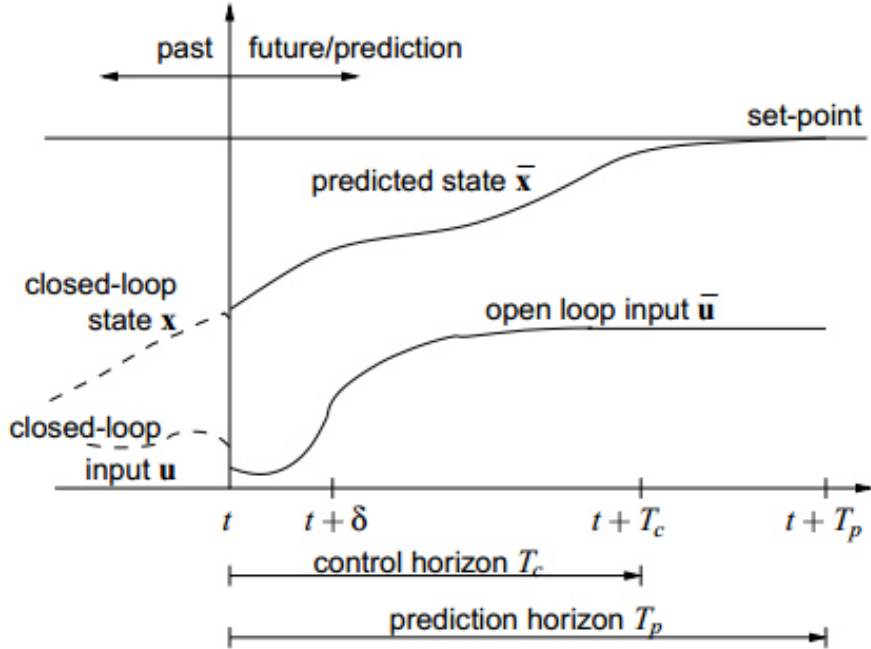


Figure 3.2: Principle of Model Predictive Control

Figure 3.2 represents the principle of a MPC, also known as a Receding Horizon Control. The controller, based on measurements obtained at a time  $t$ , will predict the future behavior of the system through a simulated plant model, over an output (prediction) horizon of size  $T_p$  and will determine, over an input (control) horizon  $T_c << T_p$ , the input that solves a predetermined open-loop optimal control problem. At time  $t + 1$  the system takes new measurements and repeats the optimization, and so on. This allows for the introduction of feedback into the system, making it able to compensate for disturbances and possible model mismatches.

### 3.2.1 Linear MPC

To clarify the MPC formulation problem, taken from [20], the next model  $\sigma$  of a system to be controlled is described by the following linear discrete time equations:

$$\sum : \begin{cases} x(t+1) = Ax(t) + Bu(t), & x(0) = x_0 \\ y(t) = Cx(t) \end{cases} \quad (3.1)$$

where  $x(t) \in \mathbb{R}^n$ ,  $u(t) \in \mathbb{R}^m$ ,  $y(t) \in \mathbb{R}^p$  refer to the state, control input and output respectively. The optimal control problem associated with the MPC scheme can be stated as follows:

$$\begin{aligned} \text{Problem}_{[t,t+T_p]} \rightarrow \text{Minimize} \quad & J(x, u), \quad x = x(s), \quad s \in [t, t+T_p] \\ \text{subject to} \quad & \dot{x}(s) = Ax(s) + Bu(s) \\ & x(t) = x_t \in C_I \subset \mathbb{R}^n \\ & x(t+T_p) \in C_F \\ & u \in \mathcal{U} := \{u : [t, t+T_p] \rightarrow \Omega : u \in L'\}, \quad \Omega \subset \mathbb{R}^n \end{aligned}$$

where:

$$\text{subject to} \begin{cases} Ex \leq F \\ Gx + Hu \leq J \end{cases} \quad (3.2)$$

Apart from these, the system has also specific stability constraints. Compared to what was shown in Figure 3.2,  $T_p$  refers to prediction horizon and  $T_c$  refers to the control horizon. A way to guarantee stability for the system, as well as a closer connection with classical optimal control methods is for example to use a prediction horizon of  $T_p = \infty$ . For the problem to be meaningful, it is assumed that  $\{(x, u) : Ex \leq F, Gx + Hu \leq J\}$  contains the origin ( $x = 0, u = 0$ ) and the mentioned stability constraints are inserted into the optimization to guarantee the close-loop.

Having this formulation concluded, the algorithm that solves the MPC scheme is as follows:

1. Initialize with  $t = t_i$  and get state  $x(t_i)$ ;
2. Solve the optimization problem over  $[t_i, t_i + T_p]$  to obtain the optimal reference trajectory  $x^*$  in this interval;
3. Compute and apply an optimal feedback control  $u^*$  during  $[t_i, t_i + T_c]$  to track  $x^*$  restricted to the control interval;
4. Sample the state variable  $x$  at  $t_i + T_c$  to obtain  $\bar{x} = x(t_i + T_c)$ ;
5. Slide the time horizon by  $T_c$  time units, define  $x(t_i) = \bar{x}$  and return to step 2;

In Figure 3.3, a block scheme of a MPC is presented, which englobes the previous concepts:

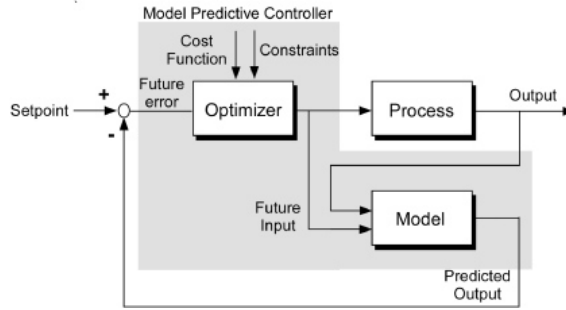


Figure 3.3: Block Diagram of a Model Predictive Controller

For additional information on Model Predictive Control, the studies presented in [21], [22] and [20] are quite valuable and extensive and thus recommended.

### 3.2.2 Nonlinear MPC

For this project, the system will follow a nonlinear model so it is also necessary to present how Model Predictive Control is adapted to deal with this type of systems. Although, a relatively new concept, several different industries are embracing this type of controller (from now on referred as NMPC), and several studies were conducted to study this control.

Due to the concise and clear information presented in [23], this section will be mostly based on this book. For further documentation on NMPC, please refer to [24] and [25].

#### 3.2.2.1 Mathematical Formulation of NMPC

Consider the stabilization problem for the class of system that can be described by the following set of differential equations:

$$\dot{x}(t) = f(x(t), u(t)), x(0) = x_0 \quad (3.3)$$

subject to the input and state constraints of the form:

$$u(t) \in \mathcal{U}, \forall t \geq 0, x(t) \in \chi, \forall t \geq 0 \quad (3.4)$$

where  $x(t) \in \chi \subseteq \mathbb{R}^n$  and  $u(t) \in \mathcal{U} \subseteq \mathbb{R}^m$  denotes the vector of states and inputs respectively. Assume that the set of input values is denoted by  $\mathcal{U}$  and the set of states is denoted by  $\chi$ , and that both satisfy the following assumptions:

1.  $\mathcal{U} \subset \mathbb{R}^p$  is compact,  $\chi \subseteq \mathbb{R}^m$  is connected and  $(0,0) \in \chi \times \mathcal{U}$ .

In its simplest form  $\mathcal{U}$  and  $\chi$  are given by box constraints of the form:

$$\mathcal{U} := \{u \in \mathbb{R}^m | u_{min} \leq u \leq u_{max}\} \quad (3.5)$$

$$\chi := \{x \in \mathbb{R}^n | x_{min} \leq x \leq x_{max}\} \quad (3.6)$$

With  $u_{min}$ ,  $u_{max}$ ,  $x_{min}$  and  $x_{max}$  as given constant vectors.

2. The vector field  $f : \mathbb{R}^n \times \mathbb{R}^m \rightarrow \mathbb{R}^n$  is continuous and satisfies  $f(0,0) = 0$ , being also locally *Lipschitz* continuous in  $x$ .
3. The system 3.3 has an unique continuous solution for any initial condition in the region of interest and any piecewise continuous and right continuous input function  $u(\cdot) : [0, T_p] \rightarrow \mathcal{U}$ .

Please remember that  $T_p$  and  $T_c$  refer to the prediction and control horizons (respectively) previously mentioned (with  $T_c < T_p$ ). To distinguish between the real system and the plant model (prediction) within the controller used , the internal variables in the controller will henceforth be represented by  $\bar{x}$  and  $\bar{u}$ , given that the predicted values, even in the nominal undisturbed case will generally not be the same as the actual closed-loop values, since the optimal input is recalculated at every sampling instance.

The finite horizon open-loop optimal control problem described can be mathematically formulated as follows:

- **Problem** Find  $\min_{\bar{u}(\cdot)} J(x(t), \bar{u}(\cdot); T_p)$

with

$$J(x(t), \bar{u}(\cdot); T_p) := \int_t^{t+T_p} F(\bar{x}(\tau), \bar{u}(\tau)) d\tau \quad (3.7)$$

subject to:

$$\dot{\bar{x}}(\tau) = f(\bar{x}(\tau), \bar{u}(\tau)), \quad \bar{x}(t) = x(t) \quad (3.8)$$

$$\bar{u}(\tau) \in \mathcal{U}, \forall \tau \in [t, t + T_c] \quad (3.9)$$

$$\bar{x}(\tau) \in \chi, \forall \tau \in [t, t + T_p] \quad (3.10)$$

The following function  $F$ , specifies the desired control performance that can arise. The standard quadratic form is the simplest and most often used one:

$$F(x, u) = (x - x_s)^T Q (x - x_s) + (u - u_s)^T R (u - u_s) \quad (3.11)$$

where  $x_s$  and  $u_s$  denote the specific set points and  $Q$  and  $R$  denote positive definite, symmetric weighting matrices. For the desired reference  $(x_s, u_s)$  to be a feasible solution for the previously stated Problem,  $u_s$  should be contained in the interior of  $\mathcal{U}$ . As stated in the second assumption, consider that  $(x_s, u_s) = (0, 0)$  is the steady state that should be stabilized.

The MPC scheme for the NMPC is similar to the one described for the linear case, presented previously on this chapter (p.24).

### 3.2.2.2 Properties of NMPC

The best case scenario would be to use infinite prediction and control horizons (setting  $T_p$  and  $T_c$  to  $\infty$ ), in order to minimize the performance objective determined by the cost. However, the open-loop optimal control problem, required to be solved online, is often formulated in a finite horizon manner and the input function is parameterized finitely, to allow a real-time numerical solution of the nonlinear open-loop optimal control problem. It becomes clear that the shorter the horizon, the less costly the solution of the online optimization problem will be. On the other hand, when using finite prediction horizons, the closed-loop input and state trajectories will differ from the predicted open-loop trajectories. In the following Figure 3.4, this can be seen, as the system can only move inside the grey area as state constraints of the form  $x(\tau) \in \chi$  are assumed:

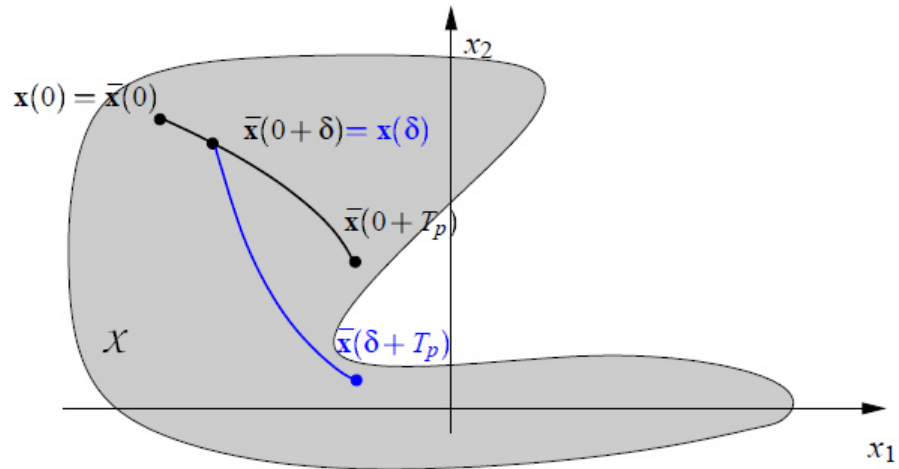


Figure 3.4: Difference between open-loop prediction and closed-loop behavior [5]

This presents the difference between standard control strategies, where the feedback law is obtained a priori and NMPC where the feedback law is obtained online with the following immediate consequences:

1. The goal to compute a feedback, such that the performance objective over the infinite horizon of the closed loop is minimized, is not achieved. A repeated minimization over a finite horizon objective in a receding horizon manner won't necessarily lead to an optimal solution for the infinite horizon problem.
2. If the predicted and actual trajectories differ, there is no guarantee that the closed-loop system will be stable.

In Figure 3.5, the overall basic structure of a NMPC control loop is presented:

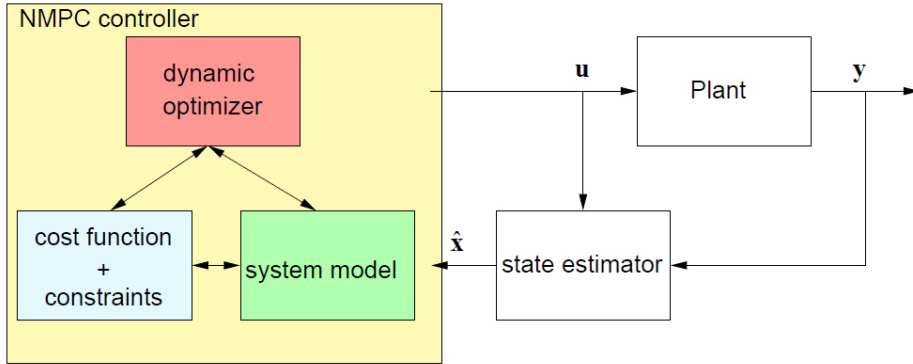


Figure 3.5: Basic NMPC Control Loop [5]

As it can be seen, it is similar to the one of a MPC, as presented before and follows the same scheme of action. From all these considerations and from the NMPC setup, the following key characteristics are extracted:

- Allows the use of a nonlinear model for prediction;
- Allows the explicit consideration of state and input constraints;
- Specified performance criteria is minimized on-line;
- The predicted behavior is in general different from the closed loop behavior;
- The on-line solution of an open-loop optimal control problem is necessary for the application of NMPC;
- To perform the prediction the system states must be measured or estimated.

# Chapter 4

## Anatomical Model Analysis

It is of the utmost importance to understand how a human arm works in order to understand what a prosthetic arm needs to cope with. With this in mind, the current chapter will provide a brief anatomical study on the human arm, trying to understand its composition and functionality, analyzing the type and purpose of movements involved, presenting data on the degrees of freedom (DOF) of each joint, a normal range of motion (ROF) and the analysis of the typical displacements in the joints according to a normal arm movement (hand to mouth motion).

### 4.1 Anatomy of the Arm

For the purpose of building a prosthetic limb, the initial and most important elements to consider are the functionality of the given limb and the joints associated with it which, for the human arm, are: glenohumeral joint (shoulder), elbow joint, wrist joint and the joints of the hand (including gliding joints, saddle joint for the thumb and lastly the metacarpophalangeal and interphalangeal joints). The arm segments will be considered rigid elements, that will be controlled by motors, in order to simplify the model, suppressing the individual muscles.

Given the complexity and extent of the project, the hand joints will not be studied thoroughly, due to the high level of different grip patterns possible by the human hand, considering merely the hand as an end-effector.

Another point that shall not be fully considered is the fact that the upper limb presents a key role in human locomotion, providing stability. Interesting by itself, this feature would greatly increase the complexity of this study, removing focus on the basic functionality of the arm itself that is intended to be studied.

In Figure 4.1 the structure and main regions of the arm are presented.

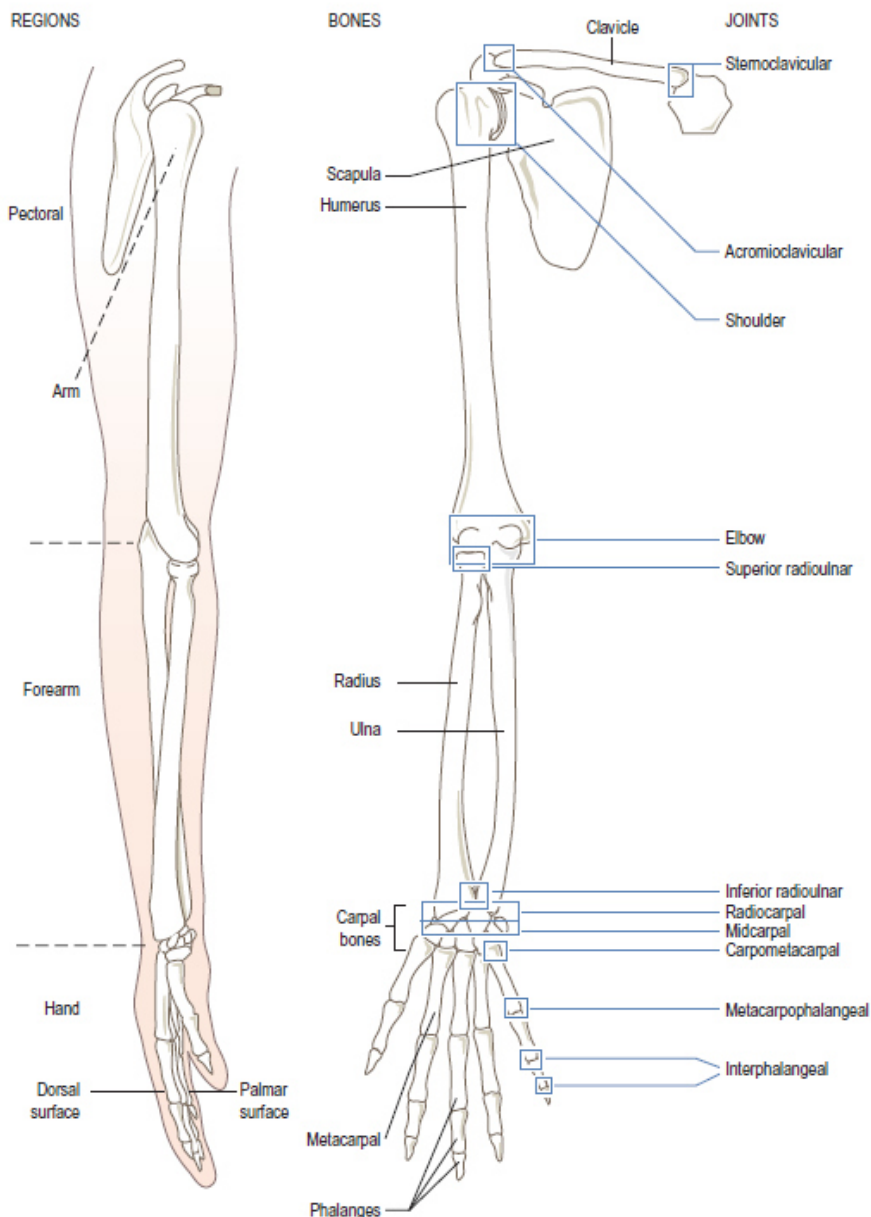


Figure 4.1: Regions, bones and joints of the arm [6]

#### 4.1.1 Average Length and Weight

The feeling of inclusion of the "external" limb is one of the most important elements of a prosthetic device. The main goal is to make the user believe that the prosthesis is not an attachment but a part of his/her own system. Considering this, it becomes important to know how the arm/forearm length and weight compare to other parts of the body to properly design the prosthetic device.

Although it improves the previously referred sense of inclusion, this element also adds complexity to the system given that a prosthetic arm will always be designed to one specific user only, given the user's required arm length and weight specifications.

The following Table 4.1 presents a comparison between average body segment lengths with the total body height of person, taken from [26].

Table 4.1: Average Body Segment Length (in percentage of Total Body Height)

<b>Segment</b>	<b>Males</b>	<b>Females</b>	<b>Average</b>
Head and Neck	10.75	10.75	10.75
Whole Trunk	30	29	29.5
Thorax	12.7	12.7	12.7
Abdomen	8.1	8.1	8.1
Pelvis	9.3	9.3	9.3
Upper Arm	17.2	17.3	17.25
Forearm	15.7	16	15.85
Hand	5.75	5.75	5.75
Thigh	23.2	24.9	24.05
Leg	24.7	25.7	25.2
Foot	4.25	4.25	4.25
Biacromial	24.5	20	22.25
Bi-iliac	11.3	12	11.65

Gathering the necessary information presented in Table 4.1, the average arm length (from shoulder to fingertip) is around 38,85 % of the average individual total body height.

Regarding weight, Table 4.2, like the one before, presents a comparison between average body segments weight and the individual total body weight, taken from [27].

Table 4.2: Average Body Segment Weight (in percentage of Total Body Weight)

<b>Segment</b>	<b>Males</b>	<b>Females</b>	<b>Average</b>
Head and Neck	6.94	6.68	6.81
Trunk	43.46	42.58	43.02
Upper Arm	2.71	2.55	2.63
Forearm	1.62	1.38	1.5
Hand	0.61	0.56	0.585
Thigh	14.16	14.78	14.47
Shank	4.33	4.81	4.57
Foot	1.37	1.29	1.33

As can be seen from Table 4.2, the average total arm weight is around 4.715 % of the average individual total body weight.

Unlike other prosthetic devices, given the kind of electronics and materials involved, a myoelectric arm prosthesis (adult arm) can weight down to a minimum of 1.010 kilograms, which is about a quarter of the weight of the arm of an average individual (about 4 kilograms). This guarantees that the user's posture will not be affected by heavy devices nor will the prosthesis be presented as a nuisance/burden to the user.

#### 4.1.2 Types of Joints and their Functionality

As seen on Figure 4.1, the human arm possesses 3 distinct joints (apart from the previously mentioned hand joints), each with very specific features and functions.

##### Shoulder Joint

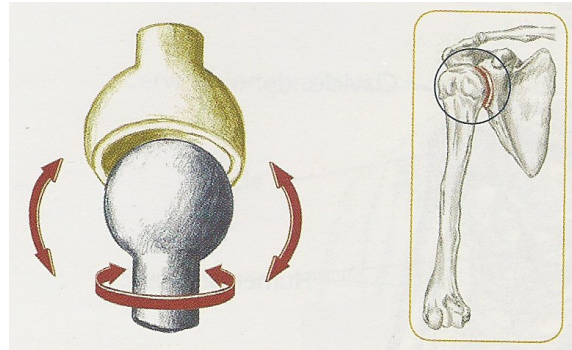


Figure 4.2: Ball and Socket Joint/Shoulder Joint [7]

Starting with the most complex one, the shoulder joint (glenohumeral joint) (Figure 4.2) is a **ball and socket joint** and, as its name clearly states, consists of the articulation between the spherical surface of a bone and a dish-shaped depression of another bone, which in case of the shoulder, represents the articulation between the humerus and the glenoid cavity.

This type of joint allows movement in every plane, involving flexion, extension, adduction and abduction (both vertical and horizontal) and medial and lateral rotation (Figure 4.3).

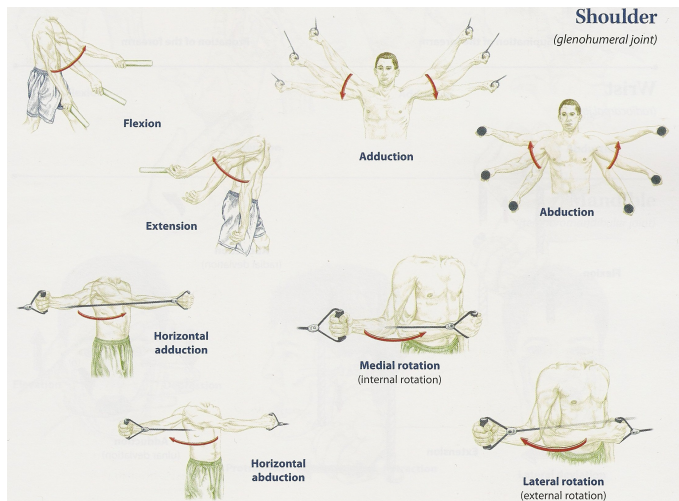


Figure 4.3: Shoulder Joint Movements [7]

This means that the shoulder joint is capable of circumduction, involving a combination of some of the previous actions, which together allow for a cone-shaped movement.

### Elbow Joint

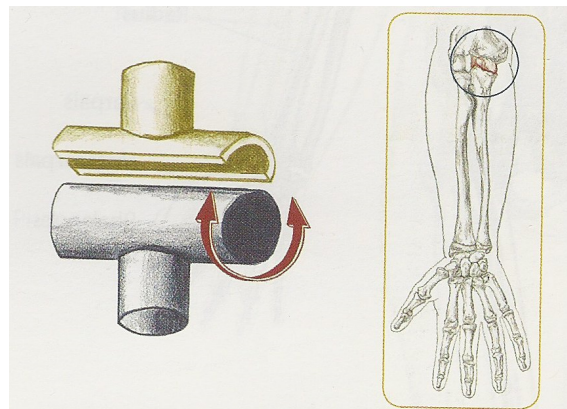


Figure 4.4: Hinge Joint/Elbow Joint [7]

Next one will be the elbow joint (humeroulnar joint), which is an **hinge joint**, as can be seen in Figure 4.4. This type of joint, as its name clearly states, provides a hinge type of movement between two body segments, which in case of the elbow connects the distal end of the humerus in the upper arm and the proximal ends of the ulna and radius in the forearm.

Unlike the glenohumeral joint, the elbow joint only allows movement in one plane due to its hinge nature. In this case, the elbow joint will allow the flexion and extension of the elbow, as can be seen in Figure 4.5.



Figure 4.5: Elbow Joint Movements [7]

Associated with the elbow joint and the forearm are two other movements: supination and pronation (Figure 4.6).

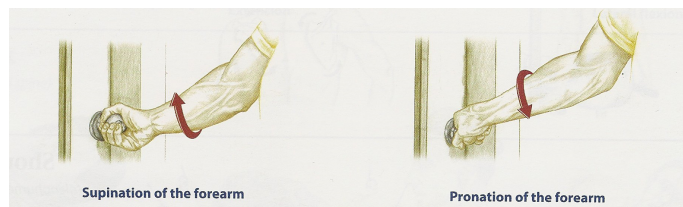


Figure 4.6: Pronation and Supination of the Forearm [7]

By the action of the pronator or supinator muscles, over the radial and ulnar bones, the forearm is able to be placed in a palm up or palm down position. This action although is not so simple to be recreated with a prosthetic device, hence the common use of hand prostheses in which the wrist itself provides a rotating mechanism, allowing to replicate the supine and pronated stances.

### Wrist Joint

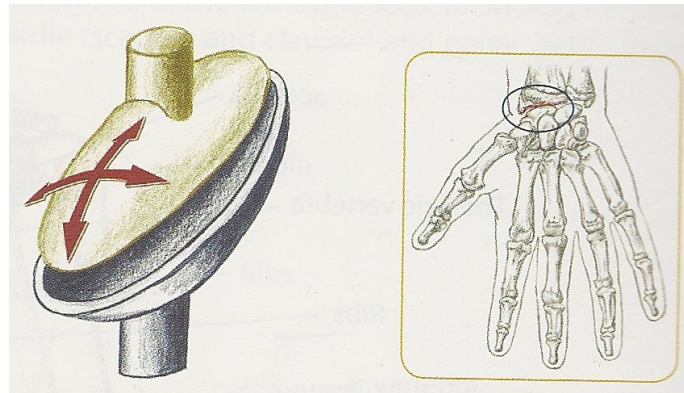


Figure 4.7: Ellipsoid Joint/Wrist Joint [7]

The last joint that will be covered in this study is the wrist joint (radiocarpal joint), which is an **ellipsoid joint**, as can be seen in Figure 4.7. This joint connects the distal part of the radial bone to the carpal bones.

As an ellipsoid joint, the wrist will allow movement in two planes, allowing flexion, extension, adduction and abduction of the joint, as can be seen in Figure 4.8.

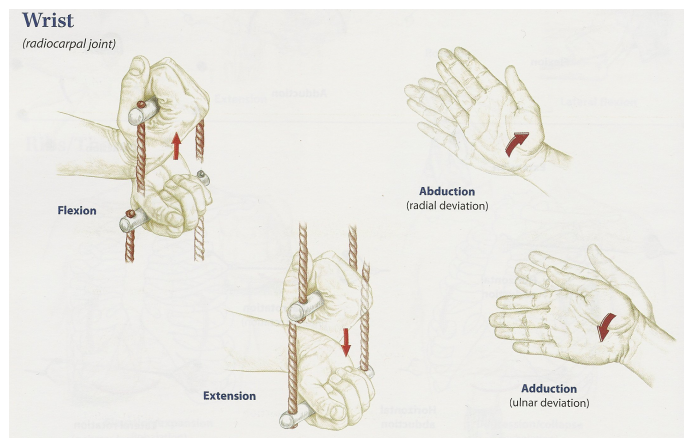


Figure 4.8: Wrist Joint Movements [7]

### 4.1.3 Range of Motion

An important aspect that has to be noted is that the previously presented joints are limited in motion. It is important to make sure that the recreated model follows these "restrictions" to correctly recreate a normal human arm type of motion.

According to the data collected present in [8], the range of motion for each degree of freedom of the joints previously mentioned is shown in Figures 4.9 and 4.10.

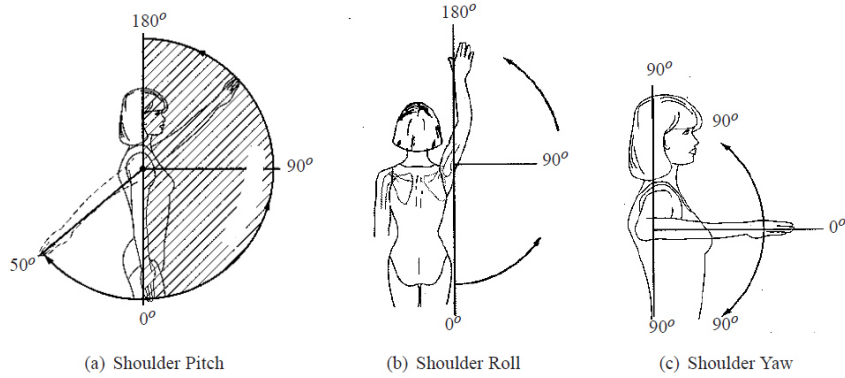


Figure 4.9: Range of Motion of Glenohumeral Joint [8]

Note that the notation presented in the figures relative to the angles is now in global coordinates (roll, pitch and yaw, respectively, rotation in x-axis, y-axis and z-axis).

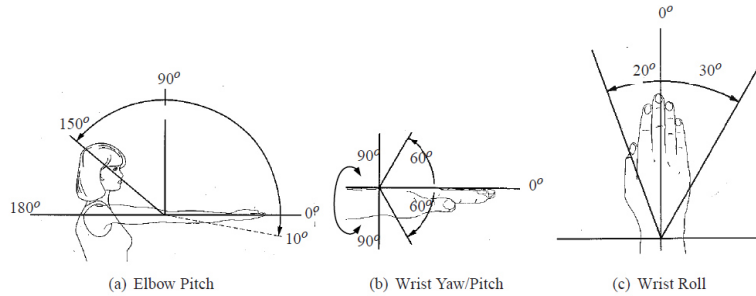


Figure 4.10: Range of Motion of Elbow and Wrist Joints [8]

The previously mentioned supination/pronation stances can be seen in Figure 4.10, recreated by the alteration of the wrist yaw.

The previous data is summarized in Table 4.3 :

Table 4.3: Range of Motion in human arm joints

Joint	Range of movement	Angle (°)
Shoulder	Pitch upper/lower	180/50
	Roll upper/lower	180/0
	Yaw upper/lower	90/90
Elbow	Pitch upper/lower	150/10
Wrist	Pitch upper/lower	60/60
	Roll upper/lower	20/30
	Yaw upper/lower	90/90

Knowing then the average length of the each arm segment, the degrees of freedom of the arm joints and lastly, the range of motion of said joints, it becomes possible to estimate a human arm's "functional workspace", as compared to normal robotic manipulators (see Figure 4.11).

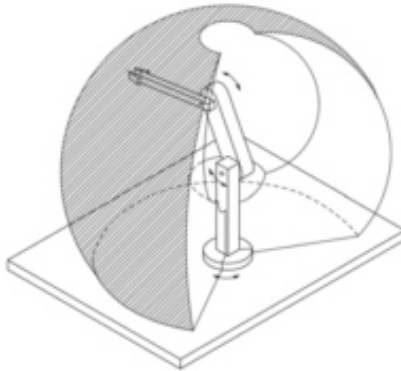


Figure 4.11: Anthropomorphic Robotic Arm Workspace [9]

It is important to estimate this functional workspace correctly in order to perform an accurate anatomical/mechanical parameters verification during the movement/action of the prosthetic device. Ideally system requires to initially estimate if the point of interest will be reachable by the prosthetic, prior to the activation of the actuators.

The work of [28] is precisely directed towards determining the human arm reachable workspace. Although the measurements present in this study slightly differ from the ones mentioned previously (arm segment measurements and range of motion), the study successfully demonstrates the workspace volume of an healthy human arm, which, for the subject used was  $V = 0.667 \pm 0.055 m^3$ . The computed workspace for said subject's right arm was then computed and is presented in Figure 4.12.

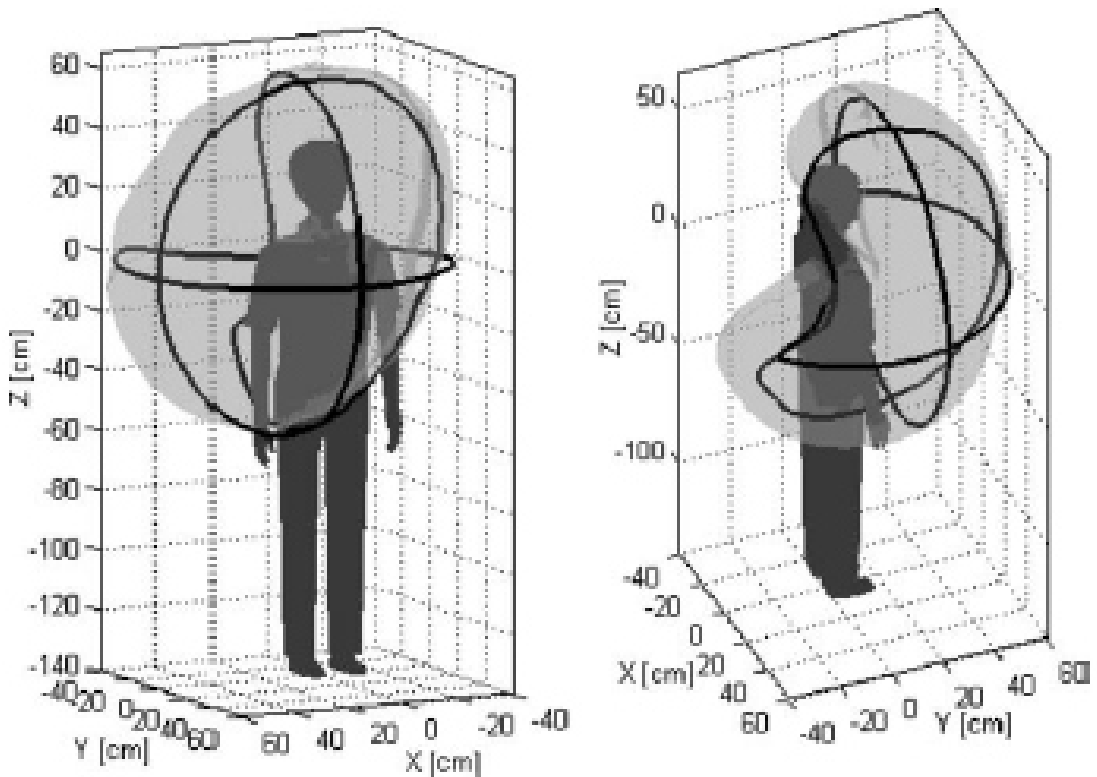


Figure 4.12: Reachable Workspace of Right Arm

The similarities between Figure 4.12 and 4.11 can now be seen. Relating this information with the desired simulation of the project, any point estipulated for the end-effector of the manipulator that is outside this volume will be discarded, forcing the user to re-plan the trajectory/plan of motion.

## 4.2 Movement Analysis

The previous sections focused on describing the characteristics and constraints of the human arm. This last section aims to present a small study on the joint displacements that occurs during a specific motion, in order to later replicate this motion in the simulation.

There are several ways to study and analyze how a body joint behaves during a certain movement and this is a field of study that has been approached for many different topics and for several years. One of the most wide spread technologies to study the joint motion is using high speed cameras (with high capture rates of several hundred frames per second, e.g. Biomechanical Laboratories) and a series of anatomically placed markers in the subject's joints being studied (an example of such placement is show in Figure 4.14). Studies like these allow for example the comprehension of how a normal or an incapacitated user reacts to specific tasks and the differences they present between each other regarding joint displacements.

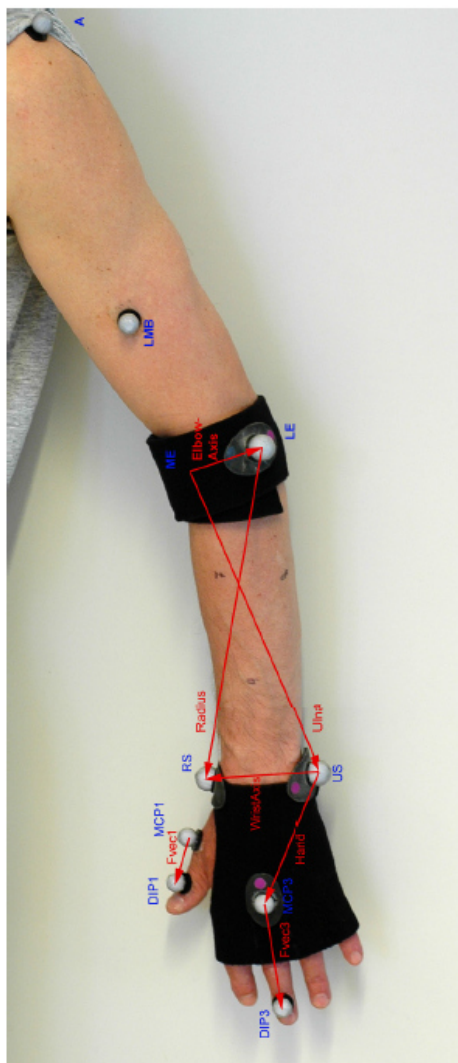


Figure 4.13: Marker placement on the upper limb [10]

As seen in Figure 4.14, there are marker clusters placed on the shoulder, elbow and wrist/hand. The subject is then asked to perform sets of specific movements over a limited period of time, during which the cameras record the actions. The data is then computed (for example with the software **Qualisys Track Manager**), identifying the location of each marker over time and withdrawing information of the joint displacements occurring for each of the 3 target areas (shoulder, elbow and wrist).

Due to the complexity of the project, it is important to select basic and easily replicated functional tasks to be performed as accurately as possible by the simulated prosthetic device. One of the studies that presented simple and interesting data is [11]. With a slight different marker configuration than that of the one present in [10], the study performed a set of different tasks with an upper limb and recorded the joint displacements. The following move set performed was selected, presenting data from an every day task (drinking or eating), in order to simulate the prosthetic movement as close to the human one analyzed.

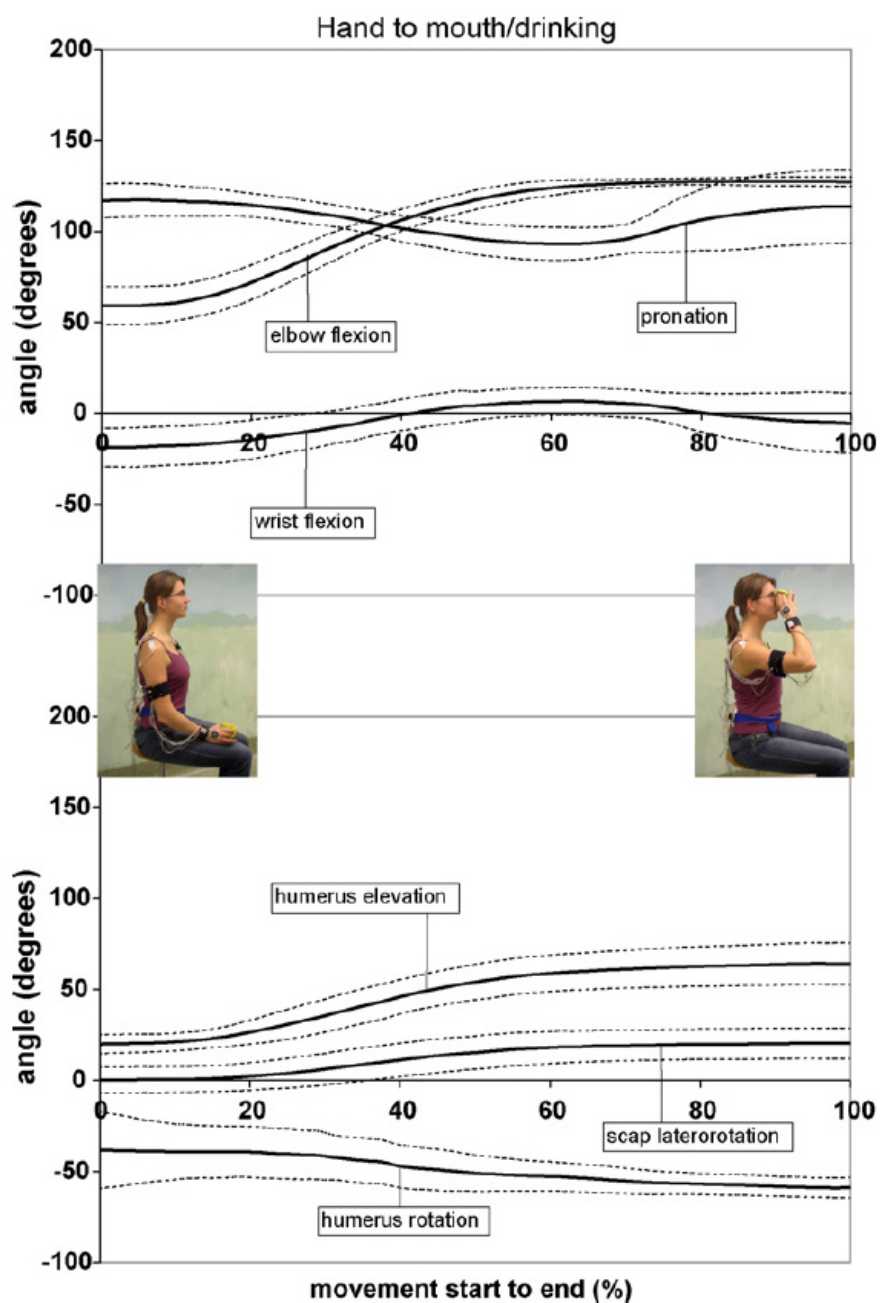


Figure 4.14: Average joint deviations during hand to mouth/drinking [11]

In the figure, the angles formed by the elbow and wrist joints are presented in the above section and the angles formed by the shoulder girdle are presented below, while the whole movement is recorded over a certain period of time (represented in the end by a certain percentage of completion instead of a time range). The filled line represents the mean between trials, while the dotted one presents the standard deviation. Regarding the forearm section (elbow and wrist joints), the positive curves correspond to a flexion or a pronating moment and the negative curves to a extension or supination moment. It is important to note that by starting the task the test subject is already grasping the object(cup) and this way, and for the purpose of the study, removing the initial grasping stage and respective movement.

## Chapter 5

# Anthropomorphic Arm Kinematic Modelling

The adopted method to design the model is based on the technique used for a normal robotic manipulator, which is using the Denavit-Hartenberg frame association, knowing the respective human arm joints and average segment lengths (as previously described on Chapter 4), performing the a Kinematic analysis.

This design and frame association was based on several biomechanical studies, namely the work presented by [29], [30], [31], [32], [9], [33] and following more in detail the model in both [34] and [12].

As mentioned in Chapter 4, an anthropomorphic arm has 7 DoF, in order to best approximate a real human limb (3 DoF in the shoulder, 1 DoF in the elbow and 3 DoF in the wrist). Please be reminded that this model does not take into consideration the several DoF that the Hand provides, merely considering a simple end-effector at the end of the wrist. Although essential and extremely interesting, the hand itself encompasses most of the upper limbs complexity in joints and functionality.

Also, it is important to mention that the 7 DoF anthropomorphic arm model is used only for the purpose of this simulation environment, given that the prosthetic arm will present a lesser number of degrees of freedom (again, not considering the hand), depending on its position. A transhumeral prosthetic device will be located bellow the shoulder, thus does not need to take into consideration the shoulder joint (and respective 3 DoF), as for a transradial prosthetic, only the forearm and the hand will be replicated.

For the purpose of the simulation the 3 DoF associated with the shoulder will be provided by the user, thus being known at all times.

An approximate schematic of the kinematic models, comparing a robotic with a human arm, is presented in [31] and can be seen in Figure 5.1.

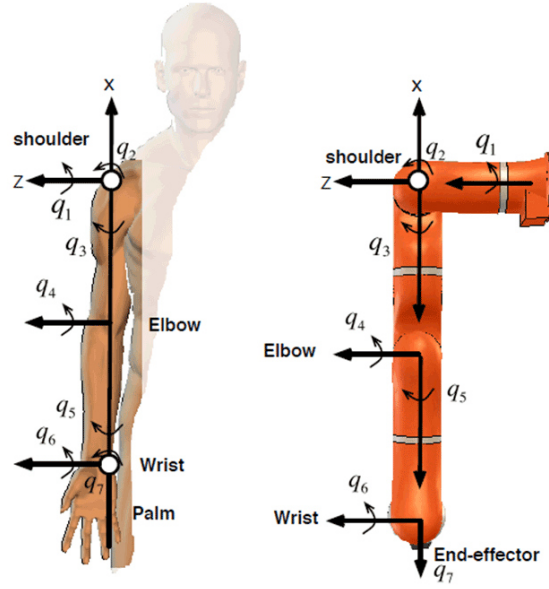


Figure 5.1: Seven DoF kinematic model of human arm and respective robotic peer

## 5.1 Kinematic Modeling

The DH method considers the system as a set of rigid bodies connected by joints with one or more DoF. To each of these DoF, the system associates a frame with specific rules to determine every axis direction. These rules, associated with a set of parameters: length ( $a_i$ ), twist ( $\alpha_i$ ), offset ( $d_i$ ) and angle ( $\theta_i$ ); describe the relationship between adjacent frames, where:

- $\alpha_i$ : angle between  $z_i$  and  $z_{i+1}$  measured about  $x_i$ ;
- $a_i$ : distance from  $z_i$  to  $z_{i+1}$  measured along  $z_i$ ;
- $d_i$ : distance from  $x_i$  to  $x_{i+1}$  measured along  $z_i$ ;
- $\theta_i$ : angle between  $x_i$  and  $x_{i+1}$  measured about  $z_i$ ;

By following these rules, the homogeneous matrix  $T_i$  is created, by the product of these four transformations:

$${}^{i-1}T_i = \text{Rot}(z, \theta_i) \text{Trans}(z, d_i) \text{Trans}(x, a_{i+1}) \text{Rot}(x, \alpha_{i+1}) \quad (5.1)$$

$${}^{i-1}T_i = \begin{bmatrix} \cos(\theta_i) & -\sin(\theta_i)\cos(\alpha_i, i+1) & \sin(\theta_i)\sin(\alpha_i, i+1) & a_{i,i+1}\cos(\theta_i) \\ \sin(\theta_i) & \cos(\theta_i)\cos(\alpha_i, i+1) & -\cos(\theta_i)\sin(\alpha_i, i+1) & a_{i,i+1}\sin(\theta_i) \\ 0 & \sin(\alpha_i, i+1) & \cos(\alpha_i, i+1) & d_i \\ 0 & 0 & 0 & 1 \end{bmatrix} \quad (5.2)$$

With this notation, any point can be expressed in another frame by following the next condition:

$${}^0A_n = {}^0T_1 \cdot {}^1T_2 \cdots {}^{n-2}T_{n-1} \cdot {}^{n-1}T_n = {}^0A_{n-1} \cdot {}^{n-1}T_n \quad (5.3)$$

In general, an homogeneous transformation takes then the form:

$$T = \begin{bmatrix} R_{3x3} & P_{3x1} \\ 0 & 1 \end{bmatrix} = \begin{bmatrix} n_x & o_x & a_x & p_x \\ n_y & o_y & a_y & p_y \\ n_z & o_z & a_z & p_z \\ 0 & 0 & 0 & 1 \end{bmatrix} \quad (5.4)$$

Where  $R_{3x3}$  represents the orientation matrix and  $P_{3x1}$  represents the position (in the cartesian space), in reference to the frame origin or, as condition 5.3 stated, to an "n" frame, if so desired.

For more information and details on kinematic modelling, please refer to [35], [30].

### 5.1.1 Forward Kinematics

Let it be understood that Forward Kinematics represents the transition from joint coordinates into cartesian coordinates. Besides the kinematic model, in [31] is also presented a study on the DH parameters fo the human arm, according to previous biomechanical research. These parameters are displayed in Table 5.1:

Table 5.1: DH parameters for a Human Arm

Frame	$\alpha_i$	$a_i$	$d_i$	$\theta_i$
1	$90^\circ$	0	0	$\theta_1$
2	$90^\circ$	0	0	$\theta_2 + 90^\circ$
3	$90^\circ$	0	$L_1$	$\theta_3 + 90^\circ$
4	$90^\circ$	0	0	$\theta_4 + 180^\circ$
5	$90^\circ$	0	$L_2$	$\theta_5 + 180^\circ$
6	$90^\circ$	0	0	$\theta_6 + 90^\circ$
7	$90^\circ$	$L_3$	0	$\theta_7 + 180^\circ$

In Table 5.1,  $L_1$ ,  $L_2$  and  $L_3$  refer to the length of the upper arm, forearm and hand segments, respectively. Let it be defined from this point on that these segment lengths are represented by  $L_u a$  (upper arm),  $L_f a$  (forearm) and  $L_h$  (hand).

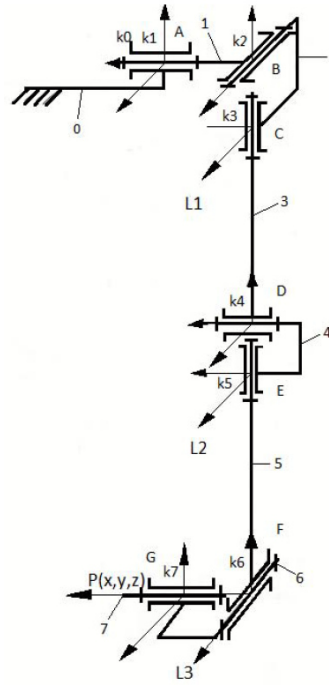


Figure 5.2: Structural scheme of a 7 DoF anthropomorphic arm [12]

Based on the previous DH parameters and the structural scheme presented in [12], shown in Figure 5.2 (considering the base frame at the shoulder), the following homogeneous matrices were constructed for each frame of the structure (see transformation and rotation matrices in the Appendix), where  $L_{ua}$ ,  $L_{fa}$  and  $L_h$  represent, respectively, the average calculated lengths of the upper arm, forearm and hand (as seen in Chapter 3):

$$H_1 = R_y(\theta_1) = \begin{bmatrix} \cos(\theta_1) & 0 & \sin(\theta_1) & 0 \\ 0 & 1 & 0 & 0 \\ -\sin(\theta_1) & 0 & \cos(\theta_1) & 0 \\ 0 & 0 & 0 & 1 \end{bmatrix} \quad (5.5)$$

$$H_2 = R_x(\theta_2) = \begin{bmatrix} 1 & 0 & 0 & 0 \\ 0 & \cos(\theta_2) & -\sin(\theta_2) & 0 \\ 0 & \sin(\theta_2) & \cos(\theta_2) & 0 \\ 0 & 0 & 0 & 1 \end{bmatrix} \quad (5.6)$$

$$H_3 = R_z(\theta_3).T_z(L_{ua}) = \begin{bmatrix} \cos(\theta_3) & \sin(\theta_3) & 0 & 0 \\ -\sin(\theta_3) & \cos(\theta_3) & 0 & 0 \\ 0 & 0 & 1 & L_{ua} \\ 0 & 0 & 0 & 1 \end{bmatrix} \quad (5.7)$$

$$H_4 = R_y(\theta_4).T_z(L_{fa}) = \begin{bmatrix} \cos(\theta_4) & 0 & \sin(\theta_4) & \sin(\theta_4).L_{fa} \\ 0 & 1 & 0 & 0 \\ -\sin(\theta_4) & 0 & \cos(\theta_4) & \cos(\theta_4).L_{fa} \\ 0 & 0 & 0 & 1 \end{bmatrix} \quad (5.8)$$

$$H_5 = R_z(\theta_5) = \begin{bmatrix} \cos(\theta_5) & \sin(\theta_5) & 0 & 0 \\ -\sin(\theta_5) & \cos(\theta_5) & 0 & 0 \\ 0 & 0 & 1 & 0 \\ 0 & 0 & 0 & 1 \end{bmatrix} \quad (5.9)$$

$$H_6 = R_x(\theta_6) = \begin{bmatrix} 1 & 0 & 0 & 0 \\ 0 & \cos(\theta_6) & -\sin(\theta_6) & 0 \\ 0 & \sin(\theta_6) & \cos(\theta_6) & 0 \\ 0 & 0 & 0 & 1 \end{bmatrix} \quad (5.10)$$

$$H_7 = R_y(\theta_7).T_y(L_h) = \begin{bmatrix} \cos(\theta_7) & 0 & \sin(\theta_7) & 0 \\ 0 & 1 & 0 & L_h \\ -\sin(\theta_7) & 0 & \cos(\theta_7) & 0 \\ 0 & 0 & 0 & 1 \end{bmatrix} \quad (5.11)$$

Having the homogeneous transformation matrices for each frame of the structure, the Forward Kinematics solution becomes available in the form of the following DH matrix of the system:

$${}^0T_7 = H_1.H_2.H_3.H_4.H_5.H_6.H_7 \quad (5.12)$$

Thus, expressing any point in the system, in relation to the base frame or any other, becomes possible by the respective adjustment and calculation of the expression 5.12.

### 5.1.2 Inverse Kinematics

Opposite to the Forward Kinematics, the Inverse Kinematics allows for the inference of the joint parameters required to provide a specific position and orientation of the end-effector (x, y, z and  $\phi_x$ ,  $\phi_y$ ,  $\phi_z$  are known).

The inverse kinematics problem is not as simple nor as linear as the forward kinematics one, having several possible approaches and sometimes multiple possible solutions. Several methods are studied and presented in [36] and [37], focusing in the use of Algebraic and Geometric solutions, specific to the problem at hand, or the use of an Iterative method, like the use Jacobian inverted matrix of the system or the CCD (cyclic coordinate descent) for simple structures. Another possible method is the use of computer software that model the manipulators (like AutoCAD) and export them to software like **Matlab's Virtual Environment**, allowing for the computation of the Inverse Kinematics through the analysis of the model itself.

In the case at hand, a geometric approached was used, based on [34], following the next steps:

1. given its nature, the robot arm has a DoF in excess of 6 possible DoF in the 3D space, so an initial condition for  $\theta_1$  (shoulder adduction/abduction) is imposed, considering this joint value known and given by the user (which doesn't pose a problem, considering that the final prosthetic limb is located anteriorly of the shoulder and it's respective joints);
2. knowing the position and orientation parameters ( $x, y, z, \phi_x, \phi_y, \phi_z$ ) a transfer matrix is created which characterizes the position and orientation of the end-effector in accordance with a fixed coordinate system;
3. using the previous transfer matrix, the wrist position is determined ( $x_w, y_w, z_w$ );
4. having then the wrist position and orientation, the remaining joint parameters will be determined ( $\theta_2 \dots \theta_7$ );

Having established the procedures, the system's transfer matrix is determined using 5.12 and the given position and orientation parameters. The matrix that then determines the wrist position and orientation is given by:

$$T_w = {}^0 T_7 * \begin{bmatrix} 1 & 0 & 0 & 0 \\ 0 & 1 & 0 & L_h \\ 0 & 0 & 1 & 0 \\ 0 & 0 & 0 & 1 \end{bmatrix}^{-1} \quad (5.13)$$

The elements of  ${}^0 T_7$  will henceforth be represented by:

$${}^0 T_7 = \begin{bmatrix} a_{11} & a_{12} & a_{13} & a_{14} \\ a_{21} & a_{22} & a_{23} & a_{24} \\ a_{31} & a_{32} & a_{33} & a_{34} \\ a_{41} & a_{42} & a_{43} & a_{44} \end{bmatrix} \quad (5.14)$$

Considering this notation, the following expression becomes valid:

$$\begin{bmatrix} a_{14} & a_{24} & a_{34} & a_{44} \end{bmatrix}^T = T_w * \begin{bmatrix} 0 & 0 & 0 & 1 \end{bmatrix}^T \quad (5.15)$$

The expression that defines the distance between the base frame and the end-effector position is:

$$d = \sqrt{a_{14}^2 + a_{24}^2 + a_{34}^2} \quad (5.16)$$

Having established these initial conditions,  $\theta_4$  is the first joint parameter that can be inferred, by following the expression:

$$\theta_4 = \pi \pm \left( \frac{L_{ua}^2 + L_{fa}^2 - d^2}{2L_u a L_{fa}} \right) \quad (5.17)$$

The formula for  $\theta_4$  is determined. Expanding Equation 5.15, the next system of equations is derived:

$$H_1.H_2.H_3.H_4. \begin{pmatrix} 0 \\ 0 \\ 0 \\ 1 \end{pmatrix} = \begin{pmatrix} a_{14} \\ a_{24} \\ a_{34} \\ 0 \end{pmatrix} \quad (5.18)$$

Multiplying this system of equations by  $A_1^{-1}$  to the right gives the following system of equations:

$$H_2.H_3.H_4. \begin{pmatrix} 0 \\ 0 \\ 0 \\ 1 \end{pmatrix} = \begin{pmatrix} b_{14} \\ b_{24} \\ b_{34} \\ 0 \end{pmatrix} \Leftrightarrow \begin{pmatrix} b_{14} \\ b_{24} \\ b_{34} \\ 0 \end{pmatrix} = A_1^{-1} \cdot \begin{pmatrix} a_{14} \\ a_{24} \\ a_{34} \\ 0 \end{pmatrix} \quad (5.19)$$

Having the value of  $\theta_4$  and the parameters from the previous system of equations, the value of  $\theta_3$  can be obtained by the following expression:

$$\theta_3 = \arccos\left(\frac{b_{14}}{L_{fa} \cdot \sin(\theta_4)}\right) \quad (5.20)$$

From Equation 5.19 and knowing both  $\theta_3$  and  $\theta_4$ , the deduction of  $\theta_2$  is performed by the following equation (where  $c(*)$  is cosine and  $s(*)$  is the sine):

$$\theta_2 = -2 \operatorname{atan}\left(\frac{L_{ua} + L_{fac}(\theta_4) + \sqrt{L_{ua}^2 + 2L_{ua}L_{fa}c(\theta_4) + (L_{fac}(\theta_4))^2 + (L_{fas}(\theta_3)s(\theta_4))^2 - b_{24}^2}}{b_{24} + L_{fa}s(\theta_3)s(\theta_4)}\right) \quad (5.21)$$

To determine the last joint parameters ( $\theta_5$ ,  $\theta_6$  and  $\theta_7$ ), the following system is considered (remembering expression 5.13):

$$H_5.H_6.H_7 = H_4^{-1}.H_3^{-1}.H_2^{-1}.H_1^{-1}.T_w \quad (5.22)$$

Let the above system be represent as:

$$H_4^{-1}.H_3^{-1}.H_2^{-1}.H_1^{-1}.T_w = \begin{pmatrix} m_{11} & m_{12} & m_{13} & m_{14} \\ m_{21} & m_{22} & m_{23} & m_{24} \\ m_{31} & m_{32} & m_{33} & m_{34} \\ m_{41} & m_{42} & m_{43} & m_{44} \end{pmatrix} \quad (5.23)$$

Through the equality of the above matrices and knowing the remaining joint parameters, the final parameters can be obtained through the following expressions:

$$\begin{cases} \theta_6 = \arcsin(m_{32}) \\ \theta_7 = -\text{atan2}(m_{31}, m_{33}) \\ \theta_5 = -\text{atan2}(m_{12}, m_{22}) \end{cases} \quad (5.24)$$

As can be seen, the system requires long and complicated calculations for determining the joint parameters, which is extremely error prone if done by hand. In order to do simplify the calculations, the whole model of the Inverse Kinematics was replicated in the tool **Simulink**, present in **Matlab**, in order for the required computation to be done fairly quick and with minimum error possible. A fraction of model implemented is presented in Figure 5.3 and 5.4, with a response time of under 50ms:

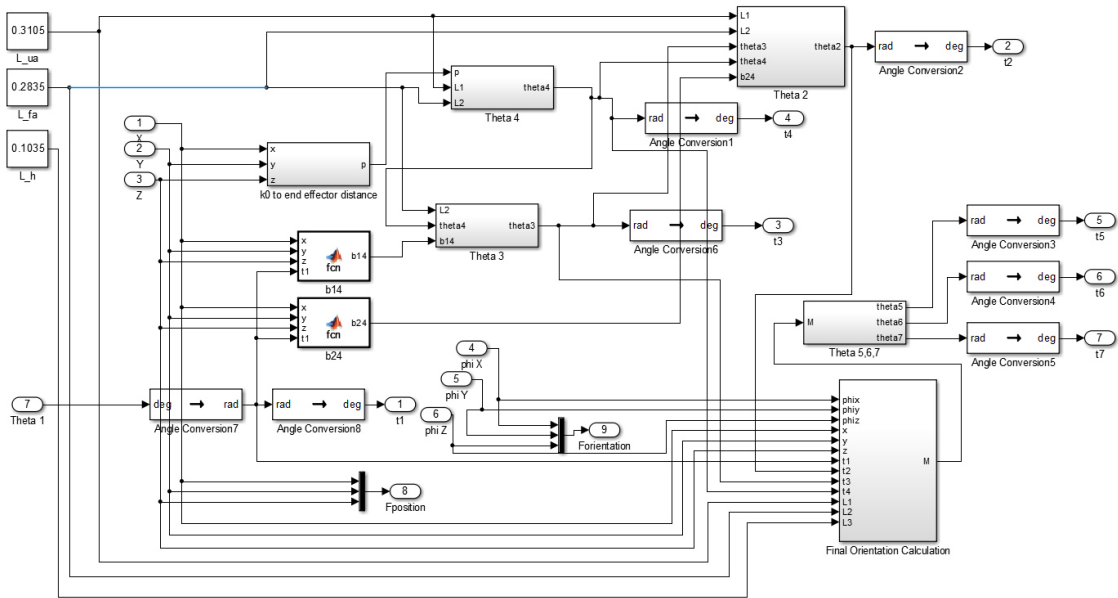


Figure 5.3: Fraction of Inverse Kinematics Simulink model

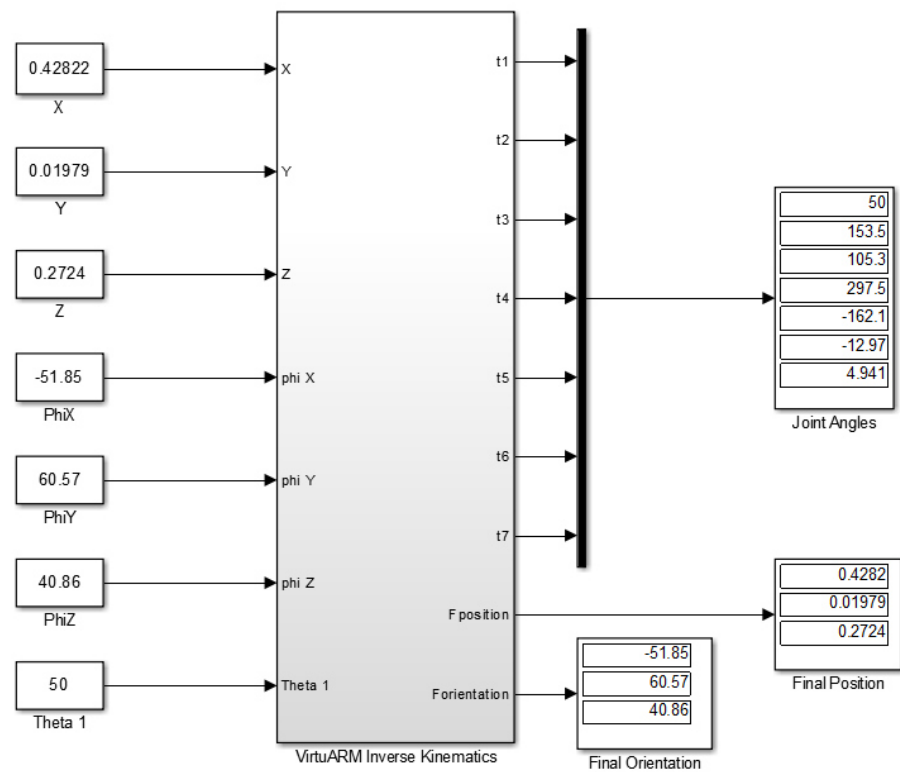


Figure 5.4: "VirtuArm" Inverse Kinematics



# **Chapter 6**

## **Problem Statement and Approach**

From the literature review concluded, plenty of information about the acquisition and processing of the MES was studied and discovered. Although, regarding the Actuators' Control itself for these prostheses (link between the detected classified types of motion and the actuators in the prosthetic device), the information discovered was vague, mostly presenting information on Finite State Machines that handle and coordinate the different motion, not mentioning the actuation and reference for each individual actuator (e.g. linear motor).

Given the high complexity of this project, with a broad range of subsystems, there is plenty of areas for improvement, since the initial debate over which features to extract and process from the MES to "feed" the Classifier, the method of Classification itself, be it using a possible ANN, a Fuzzy or any other alternative, and, as mentioned before, the Control System itself. Interesting on its own, this Classification segment wasn't integrated in the final project, again due to the limitations in time and resources.

As this project is very limited in time, and given the area of study of the author, the Control System will be the main focus.

This chapter then intends to raise the necessary project requirements, presenting an initial system concept, identifying the planned strategies to divide the overall control of the prosthetic arm into simpler subsystems and approach them with two separate levels of control (low level control with a possible Model Predictive Controller and high level control with a possible Finite State Machine).

### **6.1 Project Requirements**

Based on the reviewed literature and market survey, an initial list of requirements was established, as can be seen in Table 6.1 dividing the items between Functional and Market/User Requirements (classifying from A to C and N/A, where A is of the greater and C of lesser importance, and N is non applicable for the project at hand):

Table 6.1: Functional and Market/User Requirements

Functional Requirements	Description	Priority Level
Anatomical Accuracy	The system must respect certain anthropomorphic constraints: average human arm length and speed; joint degrees of freedom	B
Accurate MES Processing	In order to generate the correct references in the Control Architecture, the previous acquisition module must be able to correctly identify a certain desired natural motion	N
Robust and Adaptable Control	Due to the nature of this system, the control system needs to be able to quickly and effectively adapt to different situations, maintaining an accurate response	A
Instant and corrective Feedback	If a not so accurate response is obtained the system will need to perform an iterative reforing in order to obtain a close to perfect solution. In case no command is provided to the muscle, the prosthesis maintains its current position	B
Real Time Response	Given that the end user is a human being, the overall system must produce a response within 100 ms, rapid enough to make the user minimally aware of this delay	C
Market/User Requirements	Description	Priority Level
Adaptability to different individuals	A prosthetic device is something extremely personal so each product needs to have a specific size and weight for an individual user. Making a modular device which could be easily adjusted would reduce slightly the costs associated with the "personalization" of each build	N
Energy efficient	The prosthetic device encompasses a high amount of sensors and actuators that require a local battery source, making it important to bear in mind the power involved in each subsystem to maintain an acceptable battery life for the user	N
Cost efficient	Prosthetic devices in the market nowadays are highly priced due to the materials, product individuality and technology involved. Reducing the cost of manufacture is an overall must for these systems	N
Acceptable weight	The device cannot become a nuisance for the user due to overweight (usually it's considered for a myoelectric prosthesis to have around 1/4 of the weight of the user's arm, which usually corresponds to around 1 Kg)	N

## 6.2 General System Diagram

The following Figure 6.1 presents an early vision of the overall system architecture:

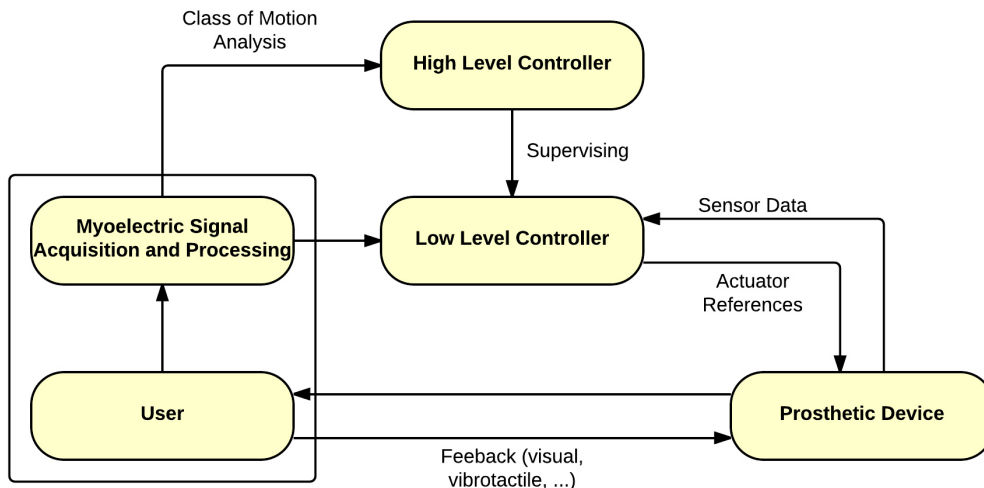


Figure 6.1: System Overview

The system is divided into four segments:

- *The user and the myoelectric acquisition system*: the responsibility of this segment is to feed the control layers the processed initial EMG signals, taking into account the verification of the anatomical and mechanical constraints, considering a targeted motion (this segment, given the goals for the project and the limited scope, will not be simulated, considering a set of known typical inputs taken from previous studies);
- *The High Level Controller*: composed by different layers, this segment is initially responsible by the decoding of the targeted motion into a motion plan with a set trajectory, feeding a motion coordination layer responsible for dividing this trajectory into separate segments for each joint, trying to approximate and adapt the signals towards a reference (natural limb motion) and for issuing the necessary commands to each of the low level controllers;
- *The Low Level Controller*: receives commands from the high level controller in order to generate and adapt the joints angle/position references for the prosthesis actuators, plus receiving information from the prosthetic sensors;
- *The prosthetic device*: with respective sensors and actuators;

### 6.3 Control Architecture

The purpose of the control architecture consists in enabling "natural" behaviors of the prosthetic arm by adapting the references made available to the low level control subsystems as the motion is being executed. The overall idea is to be able to achieve a behavior as close as possible to that of a natural normal limb with the much simpler mechanical device that embodies the prosthesis upon receiving the appropriate commands from the brain in the form of a set of EMG signals.

Let us make clear two of the ideas that stand out above:

1. **Natural Behaviors:** consists in the set of natural limb motions as a response to a certain set of "brain commands". Given the wealth of the actuators that compose a natural normal limb, as well as the rich "brain signal" content, there is a huge variety of motion behaviors which can be extremely sophisticated in the sense that extremely nuanced and subtle variations can be produced so that an overall significantly different expression can be obtained.
2. **Controller References Adaptivity:** consists in the capability of generating references to be made available to the controllers of the actuators as time evolves so that their execution is feasible within a given threshold error by the mechanical limb and, moreover, the resulting motion over time approaches that of a given natural motion.

Having presented these initial considerations, the overall control problem will now be formally stated in detail.

Let it be assumed that, from a "high level" command information, possibly extracted from "brain signals", is given a certain time horizon  $[0, T]$  and a motion reference specified by  $x_r(t)$  for all  $t \in [0, T]$ , where 0 is the time instant when motion starts,  $T$  is the time instant when the intended action is supposed to be completed and  $x_r(t)$  is the desired reference trajectory which might include positions, velocities and exerted forces at the relevant points of the natural limb.

Let it be denoted by  $x_p(t)$  the trajectory to be executed by the prosthetic arm in order to achieve the same goal in the time interval  $[0, T]$ . Given the smaller number of interconnected actuators and the consequent stricter constraints, in general, it is not possible to have a single global reference signal such that the instantaneous error ( $e(t) = \|x_r(t) - x_p(t)\|$ ) is less than some threshold  $\varepsilon_{th}$  for all  $t \in [0, T]$ .

In order to overcome this obstacle - the disparity of motion requirements between the natural and the artificial limb - the overall control system has to undertake a certain set of structural functionalities that can be organized as follows:

- (a) Replace the global reference for the natural limb by another reference formed by the concatenation of a set of suitable partial references for the artificial limb and such that the instantaneous motion error is kept within the threshold bound  $\varepsilon_{th}$
- (b) It decomposes the global reference into sub-references for each one of the actuators composing the limb in such a way that the joint constraints of all subsystems are satisfied.
- (c) It takes the feedback form in order to accommodate motion perturbations that naturally arise in real environments.

In order to achieve this functional structure, it is proposed that the overall control system is shaped by a control architecture organized into the following three levels:

- (A) **Motion Planning:** this layer of the control architecture provides the structural functionality described in item (a).
- (B) **Motion Coordination:** this layer of the control architecture provides the structural functionality described in items (b) and (c).
- (C) **Low Level Motion Execution Control:** this layer of the control architecture provides the signals for the actuators themselves.

### 6.3.1 Motion Planning

This segment, as stated before, is in charge of decoding the motion trajectory out of the targeted motion. To do so, let  $N$  be the number of segments in which the reference motion trajectory is going to be considered. This number is to be computed by a recursive procedure. Let it be given a natural reference  $x_r(\cdot)$  and an interval  $[0, T]$ . The event sequence that must take place in this stage will then be:

1. Initialization: fix  $N = 1$ .
2. For  $K = 1, \dots, N$ , solve the set of problems  $(P_K)$  with the appropriate boundary conditions and compute  $x_P^K(\cdot)$ .
3. If, for some  $t \in [0, T]$ ,  $\varepsilon(t) \leq \varepsilon_{th}$ , then the process stops, otherwise, let  $N = N + 1$  and proceed to step 2. Proceed to the formulation of the set of problems  $(P_K)$ , with  $K = 1, \dots, N$ , which have to be solved jointly.

Taking this event sequence into consideration, consider the next optimal control problem formulation, designed to solve the system for an error  $\varepsilon_N \leq \varepsilon$  (ideally as a time-continuous system, but for simplicity, represented in discrete intervals):

$$\begin{aligned}
 & \text{Minimize} && \sum_{k=0}^N \|x_{ref}(K\Delta) - x_m(K\Delta)\| \\
 & \text{subject to} && x_m((K+1)\Delta) = \bar{f}(x_m(K\Delta), u(K\Delta)) \\
 & \text{where} && u(K\Delta \in \Omega) \\
 & && J(x_m(K\Delta)) \leq 0
 \end{aligned}$$

This operation will result on the set of segments of concatenated feasible reference trajectories  $x_P^K(\cdot)$ , and their associated time intervals  $[T_{K-1}, T_K]$ ,  $K = 1, \dots, N$ , for the artificial limb.

### 6.3.2 Motion Coordination

The initial step of this segment comprises the organization of each global  $x_K^P(\cdot)$  into a set of subsystem references  $x_{P,i}^K(\cdot)$ ,  $i = 1, \dots, S$ . As mentioned in Chapter 3, the use of an MPC would prove itself valuable for the project. So, the next step involves the formulation of a global MPC problem for the optimization horizon  $[t, T_f]$ , where the global cost function is the deviation from the desired natural behavior,  $T_f$  is the updated feasible final time,  $t$  is the current time, the dynamics are given by the kinematic model presented in Chapter 5 and  $\Delta$  is the sample period.

$$\begin{aligned} \text{Problem}_{[t,t+T_p]} \rightarrow & \text{Minimize} \quad J(u, x_0) = x_t^T Q_0 x_t + \int_t^{t+T_p} [x^T(\Delta) Q x(\Delta) + u^T(\Delta) R u(\Delta)] d\Delta \\ & \text{subject to} \quad \dot{x}(\Delta) = Ax(\Delta) + Bu(\Delta) \\ & \quad x(t) = x_t \in C_I \subset \mathbb{R}^n \\ & \quad x(t + T_p) \in C_F \\ & \quad u \in \mathcal{U} := \{u : [t, t + T_p] \rightarrow \Omega : u \in L'\}, \quad \Omega \subset \mathbb{R}^n \end{aligned}$$

By solving this problem, the references for each one of the low level motion controllers in each joint from the prosthetic limb are generated.

### 6.3.3 Low Level Motion Execution Control

The last segment comprises the lowest level of the control architecture. Receiving the references generated from the above levels, each low level controller (e.g., a simple PID) will generate the position or torque references for the joint actuators of the prosthetic device.

### 6.3.4 Control Architecture Block Diagram

Having introduced all the required subsystems, the final system design is represented in Figure 6.2.

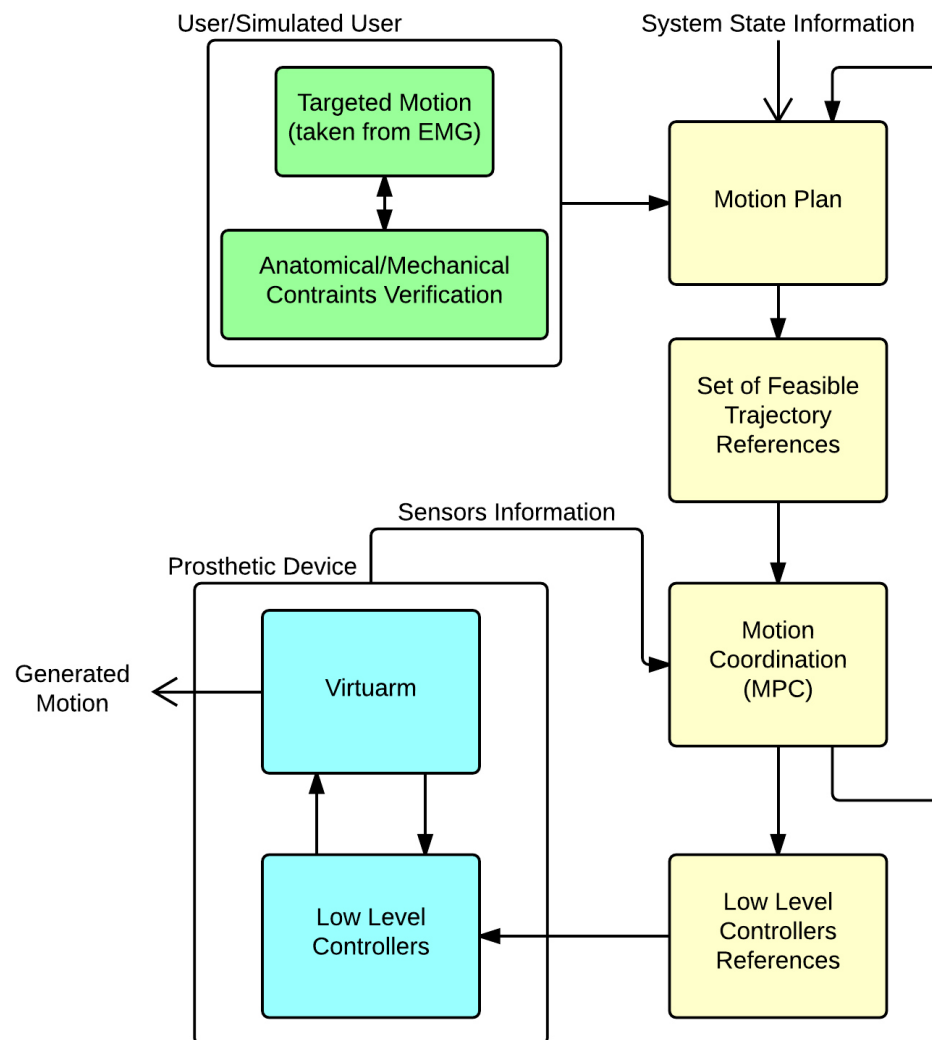


Figure 6.2: Control Architecture Diagram



# Chapter 7

## Simulated System Results

In Chapter 6, a series of subsystems were presented, each one with distinct features. Having concluded the modeling of the prosthetic limb, this current Chapter now serves the purpose to demonstrate the obtained results of simulated subsystems, from the Anatomical and Mechanical Constraints Verification to the implemented controllers responses.

### 7.1 Anatomical and Mechanical Constraints Verification

The purpose of this subsystem is to verify that the intended motion plan/estimated endpoint can be completed. To verify this condition, one of the possible solutions was to map, up to a certain degree of precision, the simulated prosthetic limb's functional workspace.

To do so, a function was created, using the Forward Kinematics model presented in Chapter 6 and the segments lengths and RoM presented in Chapter 3, to create a "cloud" of possible points for the end-effectors position of the prosthetic limb. Said function is explained in detail in the Appendix.

The results of said simulation are presented in Figures 7.1, 7.2 and 7.3.

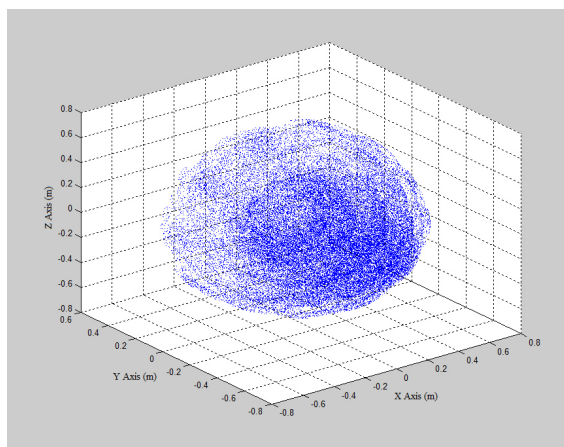


Figure 7.1: Simulated Prosthetic's Workspace - Distal Perspective

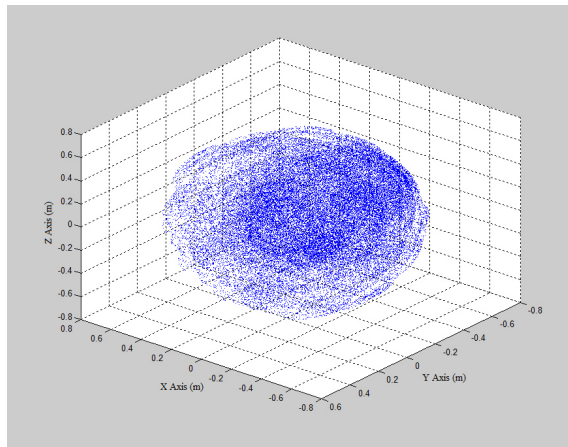


Figure 7.2: Simulated Prosthetic's Workspace - Proximal Perspective

Each dot in these graphs represents a valid target point for the end-effector, by means of a combination of plausible joint angle values for said joints. Note that the different concentrations of points in these Figures represent increased possibility of solutions, where the same point can be reached with different joint configurations. The higher concentrated areas thus represent a higher likelihood to find a reachable point.

The similarities between the manipulator's and the right human arm's functional workspace present in Chapter 4 are evident, as was intended.

After the mapping the function exports all these values into a data table, which is then used as an oracle to verify if the intended estimated positions are reachable (Figure 7.5).

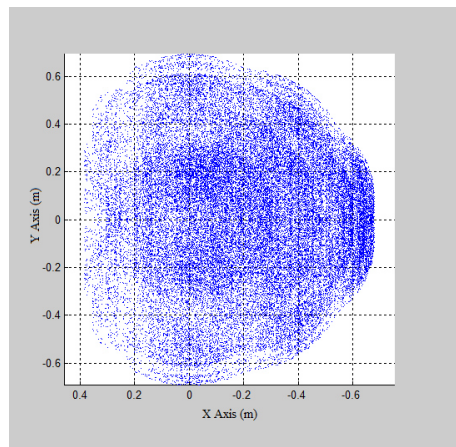


Figure 7.3: Simulated Prosthetic's Workspace Two Dimensional Overview

	A	B	C
1	X	Y	Z
2	-0,38723	0,10019	0,44193
3	-0,43302	0,073666	0,47787
4	-0,48596	0,037805	0,47605
5	-0,52582	0,0063077	0,43719
6	-0,53739	-0,0087951	0,37611
7	-0,51623	-0,0017345	0,31616
8	-0,38723	0,10019	0,44193
9	-0,4465	0,10639	0,46517
10	-0,50777	0,090753	0,45551
11	-0,54764	0,059255	0,41665
12	-0,55087	0,023928	0,36342
13	-0,51623	-0,0017345	0,31616
14	-0,41209	0,14234	0,40074
15	-0,44319	0,12153	0,45262
16	-0,47755	0,073092	0,47639
17	-0,50205	0,015544	0,46298
18	-0,50733	-0,029138	0,41751
19	-0,49137	-0,043886	0,35735
20	-0,41209	0,14234	0,40074
21	-0,4687	0,13761	0,43016
22	-0,51882	0,099124	0,44005
23	-0,54332	0,041576	0,42665
24	-0,53283	-0,013049	0,39506
25	-0,49137	-0,043886	0,35735
26	-0,4521	0,14893	0,35126

Figure 7.4: Excerpt of generated .csv file with end-effectors possible positions

Using this procedure, the system compares if the estimated position is present or approximate to the values of the data table, confirming the reachability of said position and allowing the system to direct itself towards it. If not, it will require that the user himself/herself adjusts his/her own position.

## 7.2 Case Study Arm Model Implemented

The implementation of the devised Control Architecture to the previously mentioned anthropomorphic arm model (Chapter 4) isn't applicable for the scope of this project, due to the high complexity of such operation. In order to test the given architecture, a new simpler kinematic model was created, based on the lecture notes [38], emulating a typical forearm prosthetic device (elbow and wrist joints only):

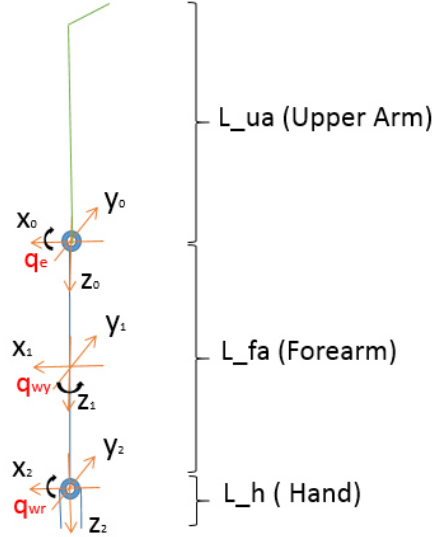


Figure 7.5: Structural scheme of a 3 DoF Forearm

The respective DH representation is then presented in Table 7.1:

Table 7.1: DH parameters for 3 DoF Forearm

Frame	$a_i$	$\alpha_i$	$d_i$	$\theta_i$
1	0	$q_e$	0	0
2	0	$q_{wr}$	$L_{fa}$	0
3	0	0	0	$q_{wy}$
4	0	0	$L_h$	0

Having computed the Forward and Inverse Kinematics equations, the following model was constructed:

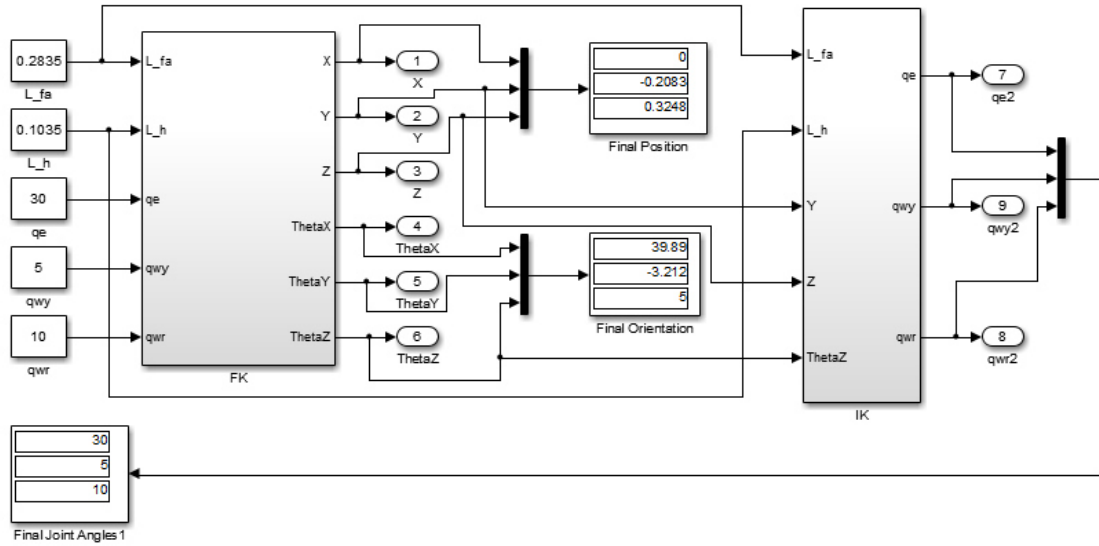


Figure 7.6: Forward and Inverse Kinematics, yielding correct results with example joint angle values

### 7.2.1 Generation of joint angle references

Having tested the kinematics model, data sets were created, replicating the joint angle deviations previously selected and demonstrated in the last section of Chapter 4.

In Figure 7.7 the trajectory taken by each of the joints is shown:

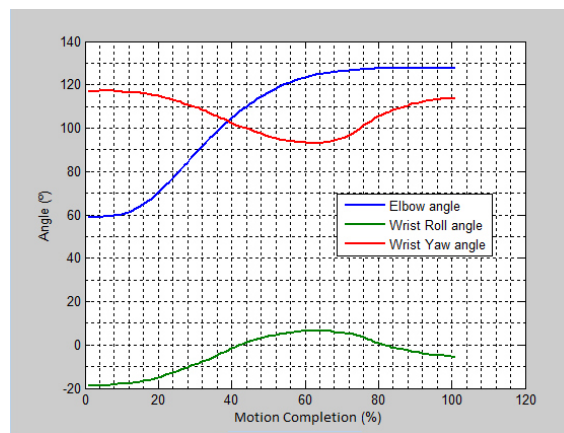


Figure 7.7: Elbow, Wrist Yaw and Wrist Roll trajectory during "drinking water" task

Having the kinematic model and the 3 joint trajectory references, a simulation of the natural movement during the "drinking water" task was performed:

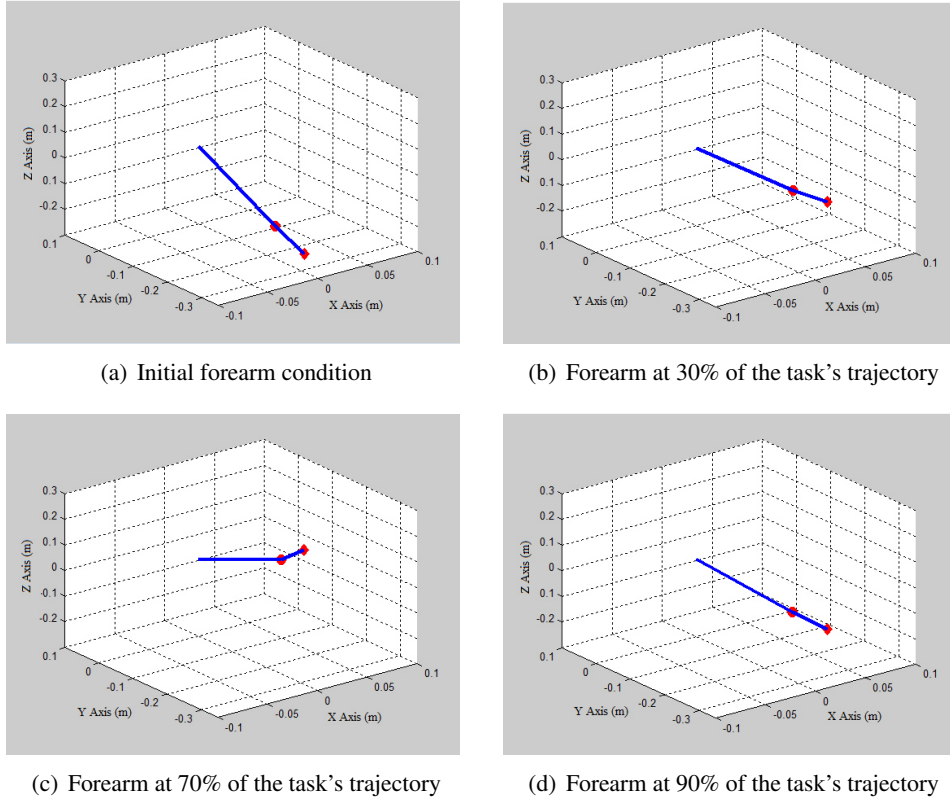


Figure 7.8: Natural trajectory of human limb during "drinking water" task

In Figure 7.8, note that the elbow is located at the origin of the referential. The line segment that connects the origin to the wrist position (represented by the red circle) represents the forearm and the line segment that connects the wrist to the tip of the end-effector (represented by the red square) represents the hand segment.

This complete motion is represented in Figure 7.9:

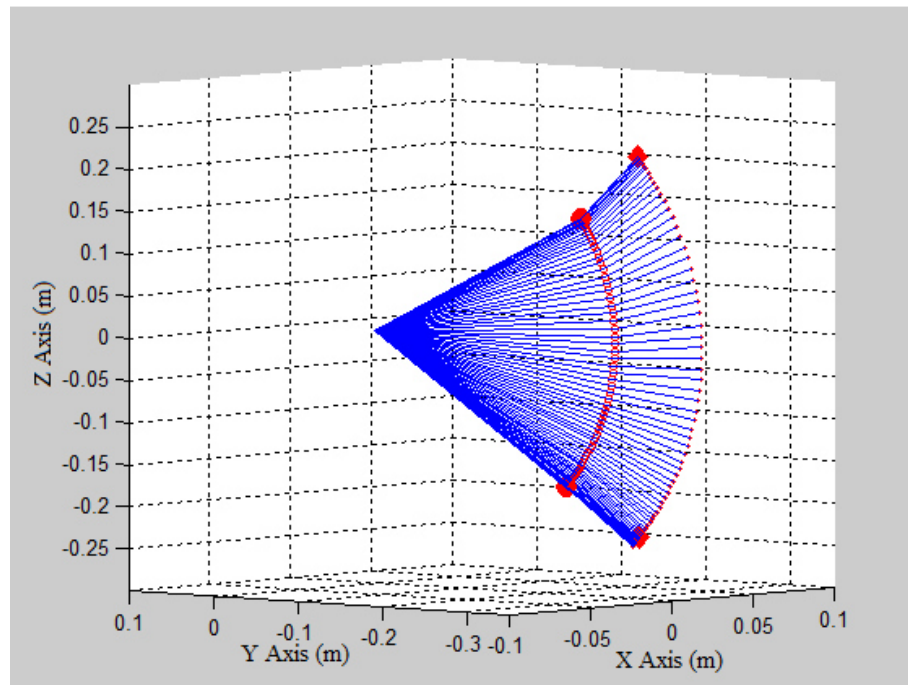
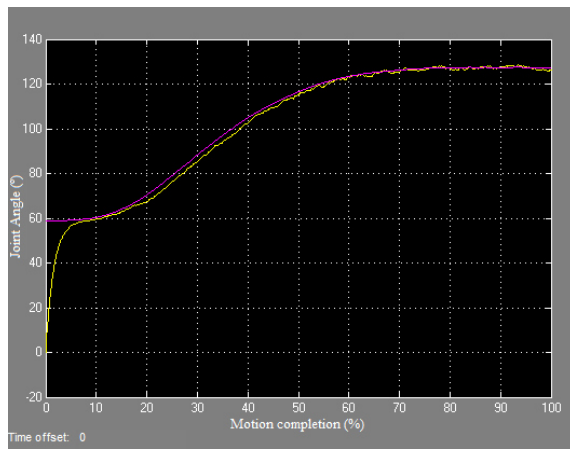


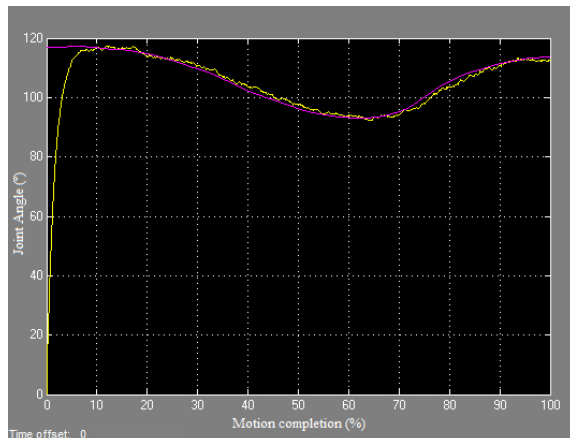
Figure 7.9: Complete "drinking water" task representation

This motion is replicated with high fidelity, demonstrating a complete natural, human-like set of movements.

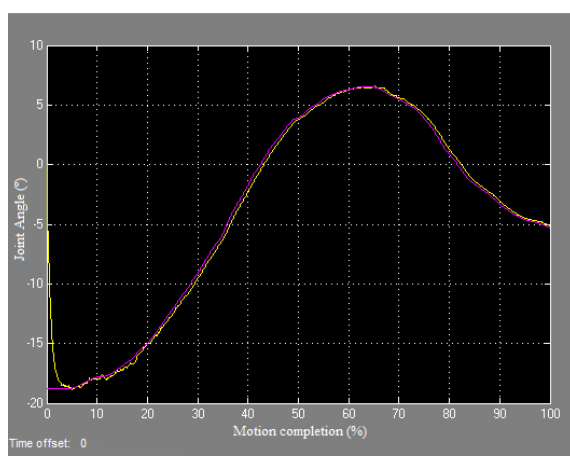
In order to test the system's response to possible external disturbances, a simulation was created to introduce a variable error factor into each respective joint angle trajectory, across several points within the trajectories themselves, having a simple PID controller attempting to correct these errors. The results, taking into consideration the case study previously mentioned, are presented in the following Figures 7.10(a), 7.10(b) and 7.10(c), where the purple line corresponds to the natural motion, intended to be replicated, while the yellow line corresponds to the controller's response to the given disturbances:



(a) Elbow joint angle trajectory approximation



(b) Wrist Yaw joint angle trajectory approximation



(c) Wrist Roll joint angle trajectory approximation

Figure 7.10: Disturbance response in "drinking water" motion task

# Chapter 8

## Conclusions

The broadness of this project revealed itself to be quite extensive, often presenting bigger and harder challenges that initially weren't fully considered.

An extensive study on Electromyography, Human Anatomy and prosthetic devices kick-started the design of a system that would be able to encompass all the human like features required to replicate an artificial limb. By analyzing State-of-the-Art technologies on EMG signal acquisition and processing, and how to use this signal to control several different devices (mostly prosthetic limbs), allowed for the inference of the project's goals and possible areas for innovation.

Conducting a medical/mechanical study on the human arm culminated in the definition of the human constraints required to be met by the artificial limb. Information on average segment lengths and weights were gathered, essential to further devise the model. Even more important, the degrees of freedom involved in each joint of the human arm (excluding hand) and respective ranges of motion were gathered. This study also allowed to understand the type of variables that would be further controlled.

To model the human arm, several studies were analyzed. In the ideal case, an anthropomorphic arm, presenting the full seven degrees of freedom, would be the best fit for such a project. Based on the work [12], the author gathered the required information to build a kinematic model of the human arm, as was presented. Later on, due to the complexity of the remaining elements of the project, the complexity of this arm model itself was reduced, altering the initial seven degrees of freedom model to one with three degrees of freedom, more adapted for the required simulations and considering the most common type of arm prosthetic device, located at a transhumeral position (forearm prosthetic). Knowing then how the model should function, being able to provide natural, human-like motion, came the need to identify which control techniques would grant an artificial limb means to be able to replicate such kind of movements. A study on nonlinear systems, hybrid control and most importantly, model predictive control was conducted, understanding how these tools could help formulate the mathematical problem behind the control of the prosthetic device.

Taking these elements into account and the respective model allowed finally for the design of a control architecture. In the authors opinion, the design of the Control Architecture presented itself to be the hardest obstacle to overcome. The definition of a high level controller based on an MPC, with the ability to adapt not only its inputs but its references as well, was the innovative factor that would approximate the prosthesis's movements as close as possible to a human limb. The design of the control architecture produced three layers - Motion Planning, Execution and Low Level Control - in which the high level controller mentioned before (integrated into the Motion Execution Layer) generates the signals for the subsystems bellow, controlling individually each joint actuator. Having both model and control, the selection of simple case study was performed, in which the simulation environment could test the controller's design. Based on the software "Matlab" the simulation of some of these elements was performed. As mentioned, the greatest difficulties of this project were in the Control Architecture. Due to lack of time, some of the elements were designed but weren't able to be fully implemented or tested, which is a key element for further developments.

As mentioned before, this project encompasses several distinct areas, ranging from the initial acquisition and processing of the EMG, to the generation of robust, quick and adaptable control signs to the prosthesis actuators. The main focus of the project was set on the model and the Control Architecture, rather than the EMG signal acquisition and processing. In this area lies a great motivation to continue this project, where real signals would be used to feed the Motion Planning block, instead of simulated ones. The use of a more accurate and with an higher degree of anthropomorphy model is one of the author's next goals. Indeed several subsystems of the project have, by themselves, related improvement areas which the author will try to explore in further developments.

# Appendix A

## Appendix

### A.1 Foward Kinematics Rotation and Translation

#### A.1.1 Translations

Translation in X, Y and Z axis, by x,y,z values respectively:

$$T_x = \begin{bmatrix} 1 & 0 & 0 & x \\ 0 & 1 & 0 & 0 \\ 0 & 0 & 1 & 0 \\ 0 & 0 & 0 & 1 \end{bmatrix}; T_y = \begin{bmatrix} 1 & 0 & 0 & 0 \\ 0 & 1 & 0 & y \\ 0 & 0 & 1 & 0 \\ 0 & 0 & 0 & 1 \end{bmatrix}; T_z = \begin{bmatrix} 1 & 0 & 0 & 0 \\ 0 & 1 & 0 & 0 \\ 0 & 0 & 1 & z \\ 0 & 0 & 0 & 1 \end{bmatrix}$$

#### A.1.2 Rotations

Rotation in X, Y and Z axis, by  $\phi_x, \phi_y, \phi_z$  degrees/radians respectively:

$$R_{\phi_x} = \begin{bmatrix} 1 & 0 & 0 & 0 \\ 0 & \cos(\phi_x) & -\sin(\phi_x) & 0 \\ 0 & \sin(\phi_x) & \cos(\phi_x) & 0 \\ 0 & 0 & 0 & 1 \end{bmatrix}; R_{\phi_y} = \begin{bmatrix} \cos(\phi_y) & 0 & \sin(\phi_y) & 0 \\ 0 & 1 & 0 & 0 \\ -\sin(\phi_y) & 0 & \cos(\phi_y) & 0 \\ 0 & 0 & 0 & 1 \end{bmatrix}$$

$$R_{\phi_z} = \begin{bmatrix} \cos(\phi_z) & -\sin(\phi_z) & 0 & 0 \\ \sin(\phi_z) & \cos(\phi_z) & 0 & 0 \\ 0 & 0 & 1 & 0 \\ 0 & 0 & 0 & 1 \end{bmatrix}$$

### A.2 Functional Workspace

The following algorithm was developed to present an approximation of the manipulators functional workspace and creation of an "oracle" table for the respective constraint verification:

```

function [Workspace] = Wkspace(L1,L2,L3)
% Wkspace -> returns a "cloud" of points for the end-effector position, based
% on the previously introduced 7 DoF arm model, with the segment lengths
% intended, thus approximating up to a high degree the manipulators
% functional workspace.

% Mean value of upper arm's lenght -> L1 = 0.3105;
% Mean value of forearm's lenght -> L2 = 0.2835;
% Mean value of hand's lenght -> L3 = 0.1035;
% Mean value of total arm length -> LT = L1+L2+L3 = 0.6975;

% The following angles represent the total RoM (upper[p] and lower[n] values) for
% each of the arms joints {3 DoF for the shoulder - S(X to Z); 1 DoF for
% the elbow - E; 3 DoF for the wrist - W(X to Z)}.

SXP = deg2rad(180);
SXN = deg2rad(-50);
SYP = deg2rad(180);
SYN = deg2rad(0);
SZP = deg2rad(90);
SZN = deg2rad(-90);
EP = deg2rad(150);
EN = deg2rad(-10);
WXP = deg2rad(60);
WXN = deg2rad(-60);
WYP = deg2rad(20);
WYN = deg2rad(-30);
WZP = deg2rad(90);
WZN = deg2rad(-90);

% Opens a file to register the "cloud" of points recorded into an .csv type
% file
fid = fopen('fworkspace.csv','w');
filename = 'fworkspace.csv';

% Mapping of the reachable points, with a pi/5 precision (36°)
for q1 = SXN:pi/5:SXP
    for q2 = SYN:pi/5:SYP
        for q3 = SZN:pi/5:SZP
            for q4 = EN:pi/5:EP

```

```

for q5 = WXn:pi/5:WXp
for q6 = WYn:pi/5:WYp
for q7 = WZn:pi/5:WZp

x = L2*sin(q4)*(cos(q1)*cos(q3)+sin(q1)*sin(q2)*sin(q3))+
L1*cos(q2)*sin(q1)+L3*cos(q7)*(cos(q6)*(sin(q4)*(cos(q1)*cos(q3)+
sin(q1)*sin(q2)*sin(q3))+cos(q2)*cos(q4)*sin(q1))+
sin(q6)*(sin(q5)*(cos(q4)*(cos(q1)*cos(q3)+sin(q1)*sin(q2)*sin(q3))-
cos(q2)*sin(q1)*sin(q4))+cos(q5)*(cos(q1)*sin(q3)-
cos(q3)*sin(q1)*sin(q2))))+
L3*sin(q7)*(cos(q5)*(cos(q4)*(cos(q1)*cos(q3)+
sin(q1)*sin(q2)*sin(q3))-cos(q2)*sin(q1)*sin(q4))-
sin(q5)*(cos(q1)*sin(q3)-cos(q3)*sin(q1)*sin(q2)))+
L2*cos(q2)*cos(q4)*sin(q1);

y = L3*sin(q7)*(cos(q5)*(sin(q2)*sin(q4)+cos(q2)*cos(q4)*sin(q3))+
cos(q2)*cos(q3)*sin(q5))-L2*cos(q4)*sin(q2)-L1*sin(q2)+
L3*cos(q7)*(sin(q6)*(sin(q5)*(sin(q2)*sin(q4)+
cos(q2)*cos(q4)*sin(q3))-cos(q2)*cos(q3)*cos(q5))-cos(q6)*(cos(q4)*sin(q2)-
cos(q2)*sin(q3)*sin(q4)))+L2*cos(q2)*sin(q3)*sin(q4);

z = L1*cos(q1)*cos(q2)-L2*sin(q4)*(cos(q3)*sin(q1)-
cos(q1)*sin(q2)*sin(q3))-L3*cos(q7)*(cos(q6)*(sin(q4)*(cos(q3)*sin(q1)-
cos(q1)*sin(q2)*sin(q3))-cos(q1)*cos(q2)*cos(q4))+sin(q6)*(sin(q5)*(cos(q4)*(cos(q3)*sin(q1)-
cos(q1)*sin(q2)*sin(q3))+cos(q5)*(sin(q1)*sin(q3)+cos(q1)*cos(q3)*sin(q2)))-
L3*sin(q7)*(cos(q5)*(cos(q4)*(cos(q3)*sin(q1)-
cos(q1)*sin(q2)*sin(q3))+cos(q1)*cos(q2)*sin(q4))-sin(q5)*(sin(q1)*sin(q3)+cos(q1)*cos(q3)*sin(q2)))+
L2*cos(q1)*cos(q2)*cos(q4);

P = {x y z};
Workspace = plot3(x,y,z);
hold on;
dlmwrite (filename, P, 'delimiter', '\t', '-append');

```

```

    end
end
end
end
end
end
end
grid on;
fclose(fid);
end

```

## A.3 Case Study Kinematics

### A.3.1 Forward Kinematics

```

function [X, Y, Z, ThetaX, ThetaY, ThetaZ] = fk(qe, qwy, qwr)

%Average Arm Segment Lengths
L_fa = 0.2835;
L_h = 0.1035;

A1 = [1          0          0          0;
       0  cosd(qe) -sind(qe)  0;
       0  sind(qe)  cosd(qe)  0;
       0          0          0          1];

A2 = [1  0          0          0;
       0  cosd(qwr) -sind(qwr)  0;
       0  sind(qwr)  cosd(qwr)  L_fa;
       0  0          0          1];

A3 = [cosd(qwy) -sind(qwy)  0  0;
       sind(qwy)  cosd(qwy)  0  0;
       0          0          1  0;
       0          0          0  1];

A4 = [1  0  0  0;
       0  1  0  0;
       0  0  1  L_h;
       0  0  0  1];

```

```

T = A1*A2*A3;

T1 = A1*A2*A3*A4;
% End effector Position
X = [1 0 0 0]*T1*[0;0;0;1];
Y = [0 1 0 0]*T1*[0;0;0;1];
Z = [0 0 1 0]*T1*[0;0;0;1];

r11 = [1 0 0 0]*T1*[1;0;0;0];
r21 = [0 2 0 0]*T1*[0;0;0;1];

r31 = [0 0 1 0]*T1*[1;0;0;0];
r32 = [0 0 1 0]*T1*[0;1;0;0];
r33 = [0 0 1 0]*T1*[0;0;1;0];

ThetaX = atan2d(r32,r33);
ThetaY = -asind(r31);
ThetaZ = acosd(r11);
end

```

### A.3.2 Inverse Kinematics

```

function[qe,qw_yaw,qw_roll] = ik(Y,Z,ThetaZ)

%Average Arm Segment Lengths
L_fa = 0.2835;
L_h = 0.1035;

qw_roll=acosd((Y^2+Z^2-L_fa^2-L_h^2)/(2*L_fa*L_h));
qe=atand(-Y/Z)-atand((L_h*sind(qw_roll))/(L_fa+(L_h*cosd(qw_roll)))); %atan2d
qw_yaw=ThetaZ;

end

```



# References

- [1] S. Herle, S. Man, G. Lazea, C. Marcu, P. Raica, and R. Robotin. Hierarchical myoelectric control of a human upper limb prosthesis. *Robotics in Alpe-Adria-Danube Region (RAAD), 2010 IEEE 19th International Workshop on*, pages 55–60, 2010.
- [2] Alcimar Soares, Adriano Andrade, Edgard Lamounier, and Renato Carrijo. The development of a virtual myoelectric prosthesis controlled by an EMG pattern recognition system based on neural networks. *Journal of Intelligent Information Systems*, 21(2):127–141, 2003.
- [3] Mohammadreza Asghari Oskoei and Huosheng Hu. Myoelectric control systems-A survey. *Biomedical Signal Processing and Control*, 2(4):275–294, October 2007. URL: <http://linkinghub.elsevier.com/retrieve/pii/S1746809407000547>, doi:10.1016/j.bspc.2007.07.009.
- [4] John Lygeros. Lecture Notes on Hybrid Systems. *University of Patras*, 2004.
- [5] Rolf Findeisen and Frank Allgöwer. An Introduction to Nonlinear Model Control. In *21st Benelux Meeting on Systems and Control*, pages 119–141, 2002.
- [6] Nigel Palastanga, D Field, and R Soames. *Anatomy and Human Movement: Structure and Function*. Physiotherapy Essentials Series. Butterworth-Heinemann, 1998. URL: <http://books.google.pt/books?id=IeJqAAAAMAAJ>.
- [7] A Biel and R Dorn. *Trail Guide to the Body: A Hands-on Guide to Locating Muscles, Bones, and More*. Books of Discovery, 2010. URL: <http://books.google.pt/books?id=6zhZSgAACAAJ>.
- [8] N P Hamilton, W Weimar, and K Luttgens. *Kinesiology: Scientific Basis of Human Motion*. Kinesiology: Scientific Basis of Human Motion. McGraw-Hill, 2008. URL: <http://books.google.pt/books?id=hjhbtQAACAAJ>.
- [9] A. Francesconi and A. Antonello. Design of a Robotic Arm for Laboratory Simulations of Spacecraft Proximity Navigation and Docking. *Università Degli Studi Di Padova*, 2013.
- [10] Anders Lyngvi Fougner. Proportional myoelectric control of a multifunction upper-limb prosthesis. *Institutt for teknisk kybernetikk*, 2007.
- [11] Carolien J van Andel, Nienke Wolterbeek, Caroline a M Doorenbosch, DirkJan H E J Veeger, and Jaap Harlaar. Complete 3D kinematics of upper extremity functional tasks. *Gait & posture*, 27(1):120–7, January 2008. URL: <http://www.ncbi.nlm.nih.gov/pubmed/17459709>, doi:10.1016/j.gaitpost.2007.03.002.

- [12] M Crenganis, R Breaz, G Racz, and O Bologa. The inverse kinematics solutions of a 7 DOF robotic arm using Fuzzy Logic. In *Industrial Electronics and Applications (ICIEA), 2012 7th IEEE Conference on*, pages 518–523, 2012. [doi:10.1109/ICIEA.2012.6360783](https://doi.org/10.1109/ICIEA.2012.6360783).
- [13] Levi J Hargrove, Kevin Englehart, and Bernard Hudgins. A comparison of surface and intramuscular myoelectric signal classification. *Biomedical Engineering, IEEE Transactions on*, 54(5):847 – 853, 2007.
- [14] Mohammadreza Asghari Oskoei and Huosheng Hu. Support Vector Machine-Based Classification Scheme for Myoelectric Control Applied to Upper Limb. *Biomedical Engineering, IEEE Transactions on*, 55(8):1956–1965, 2008.
- [15] K Englehart, B Hudgins, P.a Parker, and M Stevenson. Classification of the myoelectric signal using time-frequency based representations. *Medical Engineering & Physics*, 21(6-7):431–438, July 1999. URL: <http://linkinghub.elsevier.com/retrieve/pii/S1350453399000661>, doi:10.1016/S1350-4533(99)00066-1.
- [16] Reza Boostani and Mohammad Hassan Moradi. Evaluation of the forearm EMG signal features for the control of a prosthetic hand. *Physiological Measurement*, 24(2):309–319, May 2003. URL: <http://stacks.iop.org/0967-3334/24/i=2/a=307?key=crossref.c8c3361c322cda3999f29eb9ee7dd556>, doi:10.1088/0967-3334/24/2/307.
- [17] Arthur T C Au and Robert F Kirsch. EMG-based prediction of shoulder and elbow kinematics in able-bodied and spinal cord injured individuals. *Rehabilitation Engineering, IEEE Transactions on*, 8(4):471–480, 2000.
- [18] S S Haykin. *Neural Networks and Learning Machines*. Pearson International Edition. Pearson Education, 1994. URL: <http://books.google.pt/books?id=KCwWOAAACAAJ>.
- [19] Christian Antfolk, Anders Björkman, Sven-Olof Frank, Fredrik Sebelius, Göran Lundborg, and Birgitta Rosen. Sensory feedback from a prosthetic hand based on air-mediated pressure from the hand to the forearm skin. *Journal of rehabilitation medicine*, 44(8):702–7, July 2012. URL: <http://www.ncbi.nlm.nih.gov/pubmed/22729800>, doi:10.2340/16501977-1001.
- [20] Alberto Bemporad and Manfred Morari. Robust model predictive control: A survey. In *Robustness in identification and control*, pages 207–226. Springer, 1999.
- [21] J B Rawlings and D Q Mayne. *Model Predictive Control: Theory and Design*. Nob Hill Pub., 2009. URL: [http://books.google.pt/books?id=3\\_rfQQAACAAJ](http://books.google.pt/books?id=3_rfQQAACAAJ).
- [22] Mark Cannon. C21 Model Predictive Control Lecture 1. *University of Oxford*, 2013.
- [23] Book of Abstracts 21st Benelux Meeting on Systems and Control. *21st Benelux Meeting on Systems and Control*, 2002.
- [24] S Joe Qin and Thomas A Badgwell. An overview of nonlinear model predictive control applications. In *Nonlinear model predictive control*, pages 369–392. Springer, 2000.
- [25] Venkateswarlu Ch. Model predictive control of nonlinear processes. In Tao Zheng, editor, *Model Predictive Control*, pages 109–141. 2010.

- [26] S. Plagenhoef, F.G. Evans, and T Abdelnour. Anatomical data for analyzing human motion. *Research Quarterly for Exercise and Sport*, (54):169–178, 1983.
- [27] Paolo de Leva. Adjustments to Zatsiorsky-Seluyanov’s Segment Inertia Parameters. *Journal of Biomechanics*, 29(9):1223–1230, 1996.
- [28] Nives Klopčar and Jadran Lenarčič. Kinematic Model for Determination of Human Arm Reachable Workspace. *Meccanica*, 40(2):203–219, April 2005. URL: <http://link.springer.com/10.1007/s11012-005-3067-0>, doi:10.1007/s11012-005-3067-0.
- [29] Mohammed Z Al-faiz. Human Arm Simulation Based on Matlab with Virtual Environment. *Iraqi Journal of Computers, Communication and Control & Systems*, 11(1):86–96, 2011.
- [30] Mohammed Reyad Abuqassem. Simulation and Interfacing of 5 DOF Educational Robot Arm. *Islamic University of Gaza*, (June), 2010.
- [31] Panagiotis Artemiadis. Closed-Form Inverse Kinematic Solution for Anthropomorphic Motion in Redundant Robot Arms. *Advances in Robotics & Automation*, 02(03), 2013. doi:10.4172/2168-9695.1000110.
- [32] Valentin Grecu, Luminita Grecu, Mihai Demian, and Gabriela Demian. A Virtual System for Simulation of Human Upper Limb. In *Proceedings of the World Congress on Engineering (WCE)*, London, UK, volume II, pages 1–5. 2009.
- [33] M. Rygaard and S. Bai. Design of Anthropomorphic Robot Arm: ARA-1. *Aalborg University*, 2008.
- [34] M Creganis, I Chera, and O Bologa. The Inverse Kinematics of an Anthropomorphic Robot Arm with Seven Degrees of Freedom. *Industrial Electronics and Applications (ICIEA), 2012 7th IEEE Conference on*, 8(2):20–25, 2012.
- [35] Lorenzo Sciavicco and Bruno Siciliano. *Modelling and control of robot manipulators*. Springer, 2000.
- [36] Samuel R Buss. Introduction to Inverse Kinematics with Jacobian Transpose , Pseudoinverse and Damped Least Squares methods. *IEEE Journal of Robotics and Automation*, 17:1–19, 2004.
- [37] Lukas Barinka and Roman Berka. Inverse Kinematics - Basic Methods. *Czech Technical University*, pages 1–10, 2002.
- [38] Paulo Costa and António Moreira. Lecture Notes - Robótica Industrial. *Faculdade de Engenharia, Universidade do Porto*, 2013.
- [39] Karim Abdel-Malek, Jingzhou Yang, Richard Brand, and Emad Tanbour. Towards understanding the workspace of human limbs. *Ergonomics*, 47(13):1386–1405, 2004. doi:10.1080/00140130410001724255.
- [40] Prof Erika Ábrahám. Modeling and Analysis of Hybrid Systems Lecture Notes. *RWTH Aachen University*, 2012.
- [41] MZ Al-Faiz and AH Miry. *Artificial Human Arm Driven by EMG Signal*. INTECH Open Access Publisher, 2012. URL: <http://cdn.intechopen.com/pdfs-wm/39325.pdf>.

- [42] Happy H. An, William I. Clement, and Benjamin Reed. Analytical inverse kinematic solution with self-motion constraint for the 7-DOF restore robot arm. *2014 IEEE/ASME International Conference on Advanced Intelligent Mechatronics*, pages 1325–1330, July 2014. URL: <http://ieeexplore.ieee.org/lpdocs/epic03/wrapper.htm?arnumber=6878266>, doi:10.1109/AIM.2014.6878266.
- [43] Alejandro Hernandez Arieta and Hiroshi Yokoi. Study on the Effects of Electrical Stimulation on the Pattern Recognition for an EMG Prosthetic Application. (16360118):6919–6922, 2005.
- [44] P.K. Artermiadis and K.J. Kyriakopoulos. EMG-Based Control of a Robot Arm Using Low-Dimensional Embeddings. *Robotics, IEEE Transactions on*, 26(2):393 – 398, 2010.
- [45] Panagiotis K Artermiadis and Kostas J Kyriakopoulos. A switching regime model for the EMG-based control of a robot arm. *IEEE transactions on systems, man, and cybernetics. Part B, Cybernetics : a publication of the IEEE Systems, Man, and Cybernetics Society*, 41(1):53–63, February 2011. URL: <http://www.ncbi.nlm.nih.gov/pubmed/20403787>, doi:10.1109/TSMCB.2010.2045120.
- [46] Per Ferdinand Bach. Myoelectric signal features for upper limb prostheses. *Institutt for teknisk kybernetikk*, 2009.
- [47] Paul Bach-y Rita and Stephen W. Kercel. Sensory substitution and the human-machine interface. *Trends in Cognitive Sciences*, 7(12):541–546, December 2003. URL: <http://linkinghub.elsevier.com/retrieve/pii/S1364661303002900>, doi:10.1016/j.tics.2003.10.013.
- [48] Thomas Bak and Roozbeh Izadi-zamanabadi. Lecture Notes - Hybrid Systems. *Aalborg University*, 2004.
- [49] Amy Blank, Allison M Okamura, and Katherine J Kuchenbecker. Identifying the Role of Proprioception in Upper-Limb Prosthesis Control : Studies on Targeted Motion. *ACM Transactions on Applied Perception (TAP)*, 7(3):15, 2010.
- [50] Amy Blank, Allison M Okamura, and Katherine J Kuchenbecker. Effects of Proprioceptive Motion Feedback on Sighted and Non-Sighted Control of a Virtual Hand Prosthesis. In *Haptic interfaces for virtual environment and teleoperator systems, 2008. haptics 2008. symposium on*, number March, pages 141 – 142. 2008.
- [51] Hanneke Bouwsema, Corry K van der Sluis, and Raoul M Bongers. Learning to control opening and closing a myoelectric hand. *Archives of physical medicine and rehabilitation*, 91(9):1442–6, September 2010. URL: <http://www.ncbi.nlm.nih.gov/pubmed/20801265>, doi:10.1016/j.apmr.2010.06.025.
- [52] M Chiara Carrozza. On the Shared Control of an EMG-Controlled Prosthetic Hand : Analysis of User – Prosthesis Interaction. *IEEE Transactions on Robotics*, 24(1):170–184, 2008.
- [53] Patrick E Crago, Ning Lan, Peter H Veltink, James J Abbas, and Carole Kantor. New control strategies for neuroprosthetic systems. *Journal of Rehabilitation Research & Development*, 33(2):158–172, 1996.

- [54] Gurpreet Singh Dhillon and Kenneth W Horch. Direct neural sensory feedback and control of a prosthetic arm. *IEEE transactions on neural systems and rehabilitation engineering : a publication of the IEEE Engineering in Medicine and Biology Society*, 13(4):468–72, December 2005. URL: <http://www.ncbi.nlm.nih.gov/pubmed/16425828>, doi: [10.1109/TNSRE.2005.856072](https://doi.org/10.1109/TNSRE.2005.856072).
- [55] Erik J Dijkstra. Upper limb project. *University of Twente*, 2010.
- [56] D S Dorcas, V A Dunfield, R N Scott, and New Brunswick. Improved myo-electric control system. *Medical and biological engineering*, 8(July 1969):333–341, 1970.
- [57] Richard F ff. Weir, Phil R Troyk, Jack F Schorsch, and Huub Maas. Implantable Myoelectric Sensors (IMESs) for Intramuscular Electromyogram Recording. *IEEE Trans Biomed Eng*, 56(1):159–171, 2009. doi: [10.1109/TBME.2008.2005942](https://doi.org/10.1109/TBME.2008.2005942). *Implantable*.
- [58] C. Fleischer, C. Reinicke, and G. Hommel. Predicting the intended motion with EMG signals for an exoskeleton orthosis controller. *2005 IEEE/RSJ International Conference on Intelligent Robots and Systems*, pages 2029–2034, 2005. URL: <http://ieeexplore.ieee.org/lpdocs/epic03/wrapper.htm?arnumber=1545504>, doi: [10.1109/IROS.2005.1545504](https://doi.org/10.1109/IROS.2005.1545504).
- [59] Anders Fougner, Oyvind Stavdahl, Peter J. Kyberd, Yves G. Losier, and Philip a. Parker. Control of upper limb prostheses: Terminology and proportional myoelectric controla review. *IEEE Transactions on Neural Systems and Rehabilitation Engineering*, 20(5):663–677, 2012.
- [60] Amartya Ganguly. Modelling of bionic arm. *Journal of Biomedical Science and Engineering*, 03(03):327–329, 2010. URL: [http://www.scirp.org/Journal/PaperDownload.aspx?paperID=1536&fileName=JBiSE20100300015\\_95591588.pdf](http://www.scirp.org/Journal/PaperDownload.aspx?paperID=1536&fileName=JBiSE20100300015_95591588.pdf), doi: [10.4236/jbise.2010.33045](https://doi.org/10.4236/jbise.2010.33045).
- [61] Angel Gil-agudo, Antonio Ama-espinosa, Ana De Los Reyes-guzmán, Alberto Bernal-sahún, and Eduardo Rocón. Applications of Upper Limb Biomechanical Models in Spinal Cord Injury Patients. *INTECH Open Access Publisher*, 2011.
- [62] Diana Guimarães. Biped Locomotion Systems Analysis , Modeling and Control. *Faculdade de Engenharia da Universidade do Porto*, 2013.
- [63] Michael a. Henson. Nonlinear model predictive control: current status and future directions. *Computers & Chemical Engineering*, 23(2):187–202, December 1998. URL: <http://linkinghub.elsevier.com/retrieve/pii/S0098135498002609>, doi: [10.1016/S0098-1354\(98\)00260-9](https://doi.org/10.1016/S0098-1354(98)00260-9).
- [64] Kenneth Horch, Sanford Meek, Tyson G Taylor, and Douglas T Hutchinson. Object Discrimination With an Artificial Hand Using Electrical Stimulation of Peripheral Tactile and Proprioceptive Pathways With Intrafascicular Electrodes. *Neural Systems and Rehabilitation Engineering, IEEE Transactions on*, 19(5):483–489, 2011.
- [65] P a Kaplanis, C S Pattichis, L J Hadjileontiadis, and V C Roberts. Surface EMG analysis on normal subjects based on isometric voluntary contraction. *Journal of electromyography and kinesiology : official journal of the International Society of Electrophysiological Kinesiology*, 19(1):157–71, February 2009. URL: <http://www.ncbi.nlm.nih.gov/pubmed/17544702>, doi: [10.1016/j.jelekin.2007.03.010](https://doi.org/10.1016/j.jelekin.2007.03.010).

- [66] H.I. Krebs, N. Hogan, W. Durfee, and H. Herr. Rehabilitation robotics, orthotics, and prosthetics. In Michael Selzer Gage, Stephanie Clarke, Leonardo Cohen, Pamela Duncan, and Fred, editors, *Textbook of Neural Repair and Rehabilitation*, pages 165–181. 2006.
- [67] Todd a Kuiken, Guanglin Li, Blair a Lock, Robert D Lipschutz, Laura a Miller, Kathy a Stubblefield, and Kevin B Englehart. Targeted muscle reinnervation for real-time myoelectric control of multifunction artificial arms. *Jama*, 301(6):619–28, February 2009. URL: <http://www.ncbi.nlm.nih.gov/article/abstract.fcgi?artid=3036162&tool=pmcentrez&rendertype=abstract>, doi:10.1001/jama.2009.116.
- [68] Frank L.Lewis, Darren M.Dawson, and Chaouki T.Abdallah. *Robot Manipulator Control Theory and Practice*. CRC Press, 2003.
- [69] Guey Lau. An Intelligent Prosthetic Hand using Hybrid Actuation and Myoelectric Control. *The University of Leeds*, 2009.
- [70] C M Light, P H Chappell, B Hudgins, and K Engelhart. Intelligent multifunction myoelectric control of hand prostheses. *Journal of Medical Engineering & Technology*, 26(4):139–146, 2002. doi:10.1080/0309190021014245.
- [71] Ren C. Luo, Tsung-Wei Lin, and Yun-Hsuan Tsai. Analytical inverse kinematic solution for modularized 7-DoF redundant manipulators with offsets at shoulder and wrist. *2014 IEEE/RSJ International Conference on Intelligent Robots and Systems*, (Iros):516–521, September 2014. URL: <http://ieeexplore.ieee.org/lpdocs/epic03/wrapper.htm?arnumber=6942608>, doi:10.1109/IROS.2014.6942608.
- [72] D J Magermans, E K J Chadwick, H E J Veeger, and F C T van der Helm. Requirements for upper extremity motions during activities of daily living. *Clinical biomechanics (Bristol, Avon)*, 20(6):591–9, July 2005. URL: <http://www.ncbi.nlm.nih.gov/pubmed/15890439>, doi:10.1016/j.clinbiomech.2005.02.006.
- [73] Paul D Marasco, Keehoon Kim, James Edward Colgate, Michael a Peshkin, and Todd a Kuiken. Robotic touch shifts perception of embodiment to a prosthesis in targeted reinnervation amputees. *Brain : a journal of neurology*, 134(Pt 3):747–58, March 2011. URL: <http://www.ncbi.nlm.nih.gov/article/abstract.fcgi?artid=3044830&tool=pmcentrez&rendertype=abstract>, doi:10.1093/brain/awq361.
- [74] Ebrahim Mattar. Advances in Robotics & Automation e \_ GRASP : Robotic Hand Modeling and Simulation Environment. *Adv Robot Autom*, 2(2):1–11, 2013. doi:10.4172/2168-9695.10001.
- [75] Robert Peter Matthew, Gregorij Kurillo, Jay J Han, and Ruzena Bajcsy. Calculating Reachable Workspace Volume for use in Quantitative Medicine. In Carsten Agapito, Lourdes and Bronstein, Michael M. and Rother, editor, *Computer Vision - ECCV 2014 Workshops*, pages 570–583. 2015.
- [76] Nima Mohajerin. Identification and Predictive Control Using Recurrent Neural Networks. *Orebro University*, 2012.
- [77] Mohammadreza Asghari Oskoei and Huosheng Hu. Adaptive myoelectric human-machine interface for video games. *2009 International Conference on Mechatronics and Automation*, pages 1015–1020, August 2009. URL: <http://ieeexplore.ieee.org/lpdocs/epic03/wrapper.htm?arnumber=5330700>.

- <http://org/lpdocs/epic03/wrapper.htm?arnumber=5246300>, doi:10.1109/ICMA.2009.5246300.
- [78] P. Parker, K. Englehart, and B. Hudgins. Myoelectric signal processing for control of powered limb prostheses. *Journal of Electromyography and Kinesiology*, 16(6):541–548, December 2006. URL: <http://www.ncbi.nlm.nih.gov/pubmed/17045489>, doi:10.1016/j.jelekin.2006.08.006.
  - [79] J. Norberto Pires. Robot Manipulators and Control Systems. In *Industrial Robots Programming*, pages 35–107. 2007. doi:10.1007/978-0-387-23326-0\\_\\_2.
  - [80] Alvaro Rios Poveda. Myoelectric prostheses with sensorial feedback. *University of New Brunswick*, 2002.
  - [81] M B I Raez, M S Hussain, and F Mohd-Yasin. Techniques of EMG signal analysis: detection, processing, classification and applications. *Biological procedures online*, 8(1):11–35, January 2006. URL: <http://www.ncbi.nlm.nih.gov/pmc/articles/1455479/>, doi:10.1251/bpo115.
  - [82] Ranjeet Ranjan, Arbin Kumar, and Praveen Dhyani. *Modeling and Simulation of Robotic Humanoid Arm*, volume 4. 2012.
  - [83] Rinku Roy, Amit Konar, D.N. Tibarewala, and R. Janarthanan. EEG driven model predictive position control of an artificial limb using neural net. In *Computing Communication & Networking Technologies (ICCCNT), 2012 Third International Conference on*, number July, pages 1 – 9. 2012.
  - [84] Kathleen Talbot. Using Arduino to Design a Myoelectric Prosthetic. *Saint John's University*, 2014.
  - [85] Federico Thomas. *Solved Problems in Robot Kinematics Using the Robotics Toolbox*. Universitat Politècnica de Catalunya, 2012.
  - [86] Deepak Tolani, Ambarish Goswami, and Norman I. Badler. Real-Time Inverse Kinematics Techniques for Anthropomorphic Limbs. *Graphical Models*, 62(5):353–388, September 2000. URL: <http://linkinghub.elsevier.com/retrieve/pii/S1524070300905289>, doi:10.1006/gmod.2000.0528.
  - [87] Quanzhao Tu, Xiafu Peng, Jiehua Zhou, and Xunyu Zhong. Kinematics Simulation and Analysis of 2-DOF Parallel Manipulator with Highly Redundant Actuation. pages 2–5, 2011.
  - [88] Huiyu Zhou and Huosheng Hu. Human motion tracking for rehabilitation—A survey. *Biomedical Signal Processing and Control*, 3(1):1–18, January 2008. URL: <http://linkinghub.elsevier.com/retrieve/pii/S1746809407000778>, doi:10.1016/j.bspc.2007.09.001.